T.C.
DOKUZ EYLUL UNIVERSITY
IZMIR INTERNATIONAL
BIOMEDICINE AND GENOME
INSTITUTE

TRANSCRIPTOMIC ANALYSIS OF THE EFFECT OF DR4/5 DEATH RECEPTOR ACTIVATION ON THE DIFFERENTIATION OF PRIMARY HUMAN MONOCYTES TO M1 MACROPHAGES

AYŞENUR ÖNER

MOLECULAR BIOLOGY AND GENETICS

MASTER OF SCIENCES THESIS

İZMİR-2022

THESIS ID: DEU.IBG.MSc.2020850013

T.C.
DOKUZ EYLUL UNIVERSITY
IZMIR INTERNATIONAL
BIOMEDICINE AND GENOME
INSTITUTE

TRANSCRIPTOMIC ANALYSIS OF THE EFFECT OF DR4/5 DEATH RECEPTOR ACTIVATION ON THE DIFFERENTIATION OF PRIMARY HUMAN MONOCYTES TO M1 MACROPHAGES

MOLECULAR BIOLOGY AND GENETICS

MASTER OF SCIENCES THESIS

AYŞENUR ÖNER

Supervisor: Assoc.Prof. DUYGU SAĞ

This study is supported by H2020 MSCA RISE Programs (Grant no #777995)

THESIS ID: DEU.IBG.MSc.2020850013

Dokuz Eylül Üniversitesi İzmir Uluslararası Biyotıp ve Genom Enstitüsü, Genom Bilimleri ve Moleküler Biyoteknoloji Anabilim Dalı, Moleküler Biyoloji ve Genetik Yüksek Lisans Programı "2020850013" numaralı öğrencisi Ayşenur ÖNER, "**DR4/5 ölüm reseptörü aktivasyonunun primer insan monositlerinin M1 makrofajlarına dönüşmesine etkisinin transkriptomik analizi**" konulu Yüksek Lisans tezinde 26/12/2022 tarihinde yapılan savunma sınavı sonucunda başarılı olmuştur.

BAŞKAN
Doç. Dr. Duygu SAĞ
Dokuz Eylül Üniversitesi
İzmir Uluslararası Biyotıp ve Genom Enstitüsü
Genom Bilimleri ve Moleküler Biyoteknoloji Anabilim Dalı

JÜRİ ÜYESİ
Doç.Dr. Gökhan KARAKÜLAH
Dokuz Eylül Üniversitesi
İzmir Uluslararası Biyotıp ve Genom Enstitüsü
Genom Bilimleri ve Moleküler Biyoteknoloji
Anabilim Dalı

JÜRİ ÜYESİ
Dr.Öğr.Üyesi Atakan EKİZ
İzmir Yüksek Teknoloji Enstitüsü
Fen Fakültesi
Moleküler Biyoloji ve Genetik Bölümü

REPORT OF THE MASTER DEGREE THESIS DEFENSE EXAM

Dokuz Eylul University Izmir International Biomedicine and Genome Institute, Department of Genomic Sciences and Molecular Biotechnology, Molecular Biology and Genetics MSc program student Ayşenur ÖNER, numbered "2020850013", successfully completed her MSc thesis defense on "**Transcriptomic analysis of the effect of DR4/5 death receptor activation on the differentiation of primary human monocytes to M1 macrophages**" on the date of 26/12/2022.

CHAIR
Assoc.Prof. Duygu SAG
Dokuz Eylul University
Izmir International Biomedicine and Genome Institute
Department of Genomic Sciences and Molecular Biotechnology

JURY MEMBER
Assoc.Prof. Gökhan KARAKÜLAH
Dokuz Eylul University
Izmir International Biomedicine and Genome Institute
Department of Genomic Sciences and Molecular Biotechnology

JURY MEMBER
Assist. Prof. Atakan EKİZ
Izmir Institute of Technology
Faculty of Science
Department of Molecular Biology and Genetics

TABLE OF CONTENT

INDEX OF FIGURES

INDEX OF TABLES

LIST OF ABBREVIATIONS

7AAD	7-Aminoactinomycin D
A2R	A2 Adenosine Receptor
Akt	Protein Kinase B
APC	Allophycocyanin
APCs	Antigen Presenting Cells
Apo-2L	Apo2 Ligand
Bcl-2	B-Cell Lymphoma 2
BFGF	Basic Fibroblast Growth Factor
bp	Base Pair
BSA	Bovine Serum Albumin
BV510	Brilliant Violet 510
c-FLIP	Cellular FLICE Inhibitory Protein
CCL	C-C Motif Chemokine Ligand
CCR	C-C Chemokine Receptor
CD	Cluster Of Differentiation
cDNA	Complementary DNA
CPM	Counts Per Million
CSF-1	Colony Stimulating Factor 1
CXCL	C-X-C Motif Chemokine Ligand
DcR	Decoy Receptor
DEGs	Differentially Expressed Genes
DISC	Death-Inducing Signaling Complex
DNA	Deoxyribonucleic Acid
dNTPs	Deoxyribonucleotide Triphosphate
DR	Death Receptor
DTT	Dithiothreitol
EAE	Encephalomyelitis
EGF	Epithelial Growth Factor
EGFR	Epithelial Growth Ligands of The Factor Receptor
ELISA	Enzyme-Linked Immunosorbent Assay
ERK	Extracellular Signal-Regulated Kinase
FACS	Fluorescence-Activated Cell Sorting
FADD	Fas-Associated Protein With Death Domain
FBS	Fetal Bovine Serum
Fc	Fragment Crystallizable
FC	Fold Change
FDR	False Discovery Rate
FIZZ1	Found in Inflammatory Zone 1
FLICE	FADD-Like Interleukin-1β Converting Enzyme
FPKM	Fragments Per Kilobase Million

GTPase	Guanosine Triphosphate (GTP) Hydrolase Enzyme
HGF	Hepatocyte Growth Factor
IBD	Inflammatory Bowel Disease
IFN-gamma	Interferon Gamma
IL	Interleukin
ILCs	Innate Lymphoid Cells
IRF	Interferon Regulatory Factor
iNOS	Inducible Nitric Oxide Synthase
jmjd3	Jumonji Domain-Containing-3
JNK	C-jun N-Terminal Kinase
LPS	Lipopolysaccharides
M-CSF	Macrophage Colony-Stimulating Factor
MAPK	Mitogen-Activated Protein Kinase
MHC	Major Histocompatibility Complex
mL	Milliliter
MMPs	Matrix Metalloproteinases
MS	Multiple Sclerosis
LncRNA	Long non-coding RNA
NF-kB	Nuclear Factor Kappa-Light-Chain-Enhancer Of Activated B Cells
ng	Nanogram
NKs	Natural Killer cells
OPG	Osteoprotegerin
PAMPs	Pathogen-Associated Molecular Patterns
PBMCs	Peripheral Blood Mononuclear Cells
PBS	Phosphate Buffered Saline
PC	Principial Component
PCA	Principial Component Analysis
PCR	Polymerase Chain Reaction
PDGF	Platelet-Derived Growth Factor
PE	Phycoerythrin
PE-Dazzle 594	Phycoerythrin Dazzle 594
PI3K	Phosphoinositide 3-Kinase
PPAR	Peroxisome Proliferator-Activated Receptors
PRRs	Pattern Recognition Receptors
PTGS2	Prostaglandin-Endoperoxide Synthase 2
qPCR	Quantitative Polymerase Chain Reaction
RA	Rheumatoid Arthritis
RCF	Relative Centrifugal Force
rh TRAIL	Recombinant Human TRAIL
RIN	RNA Integrity Number
RNA	Ribonucleic Acid

RNA-seq	RNA-Sequencing
RNAse	Ribonuclease
RPMI	Roswell Park Memorial Institute Medium
RQ	Relative Quantification
rRNA	Ribosomal Ribonucleic Acid
RSEM	RNA-Seq By Expectation-Maximization
RT	Room Temperature
RT-qPCR	Real Time
SEM	Standard Error of The Mean
STAT	Signal Transducer And Activator of Transcription
T	Treated
TAMs	Tumor-Associated Macrophages
tBid	Truncated Bh3 Interacting-Domain Death Agonist
TGF	Transforming Growth Factor
Th2	Helper T Cell
TLR	Toll-Like Receptor
TME	The Tumor Microenvironment
TMM	Trimmed Mean Of M Values
TNF	Tumor Necrosis Factor
TRAIL	TNF-Related apoptosis-inducing ligand
TRAIL-R	TRAIL Receptor
Treg	Regulatory T Cell
UT	Untreated
UV	Ultraviolet
VEGF	Vascular Endothelial Growth Factor
VSMCs	Vascular Smooth Muscle Cells
w/o	Without
xg	Relative Centrifugal Force
XIAP	X-Linked Inhibitor of Apoptosis
β-ME	2-Mercaptoethanol
µl	Microliter

ACKNOWLEDGEMENTS

I would like to express my deepest gratitude to Assoc.Prof. Duygu Sağ, my esteemed advisor, for all the guidance, support and endless love throughout my master study. She always made me feel like one of her family members and gave me so many opportunities to outgrow myself and words cannot express my gratitude to my advisor. Many thanks to generous financial support from the TÜBİTAK 2210-A scholarship. Thank you to my jury members, Assoc.Prof. Gökhan Karakülah and Assist. Prof. Atakan Ekiz for your encouraging words and thoughtful feedback.

I am also thankful to Dr. Sinem Günalp for always supporting me lovingly all the time and for always making me laugh and reminding me again how good it feels. She will always be my best friend and big sister. I am also thankful to my lab members, Göksu D. Helvacı, Dr. Duygu Ünüvar and Aslı Korkmaz who have been there for me emotionally and intellectually and have added a lot to my life. I am fortunate to have been a part of this lab group which always felt at home.

I am forever thankful to Vedat Sarı who generously support me and help me every step of the way. Thanks of course to my dear friends, Buse Korkmaz, Aslı Canbalaban, Mert Yıldız, Damla Bakaçhan, Ersin Gündeğer and Şimal Özbek for their support and friendship. Thanks should also go to Sezin Sivri and Gülhan Berkman for supporting me whenever I needed them and sparing time for me no matter what.

Lastly, my family deserves endless gratitude for always being there for me and for trusting me even if I didn’t feel that way. My accomplishments would not have been possible without them. My Deepest thanks to my little brother, Kerem, for just being so cute, just thinking about him makes me happy.

TRANSCRIPTOMIC ANALYSIS OF THE EFFECT OF DR4/5 DEATH RECEPTOR ACTIVATION ON THE DIFFERENTIATION OF PRIMARY HUMAN MONOCYTES TO M1 MACROPHAGES

Ayşenur Öner, Dokuz Eylul University, Izmir International Biomedicine and Genome Institute, Molecular Biology and Genetics, Izmir/TURKEY

ABSTRACT

TNF-related apoptosis-inducing ligand (TRAIL) is a member of the TNF family and induces either apoptosis or survival. Inducing apoptosis selectively in malignant cells without affecting normal cells makes TRAIL a promising agent for cancer therapy. Macrophages play key roles in both innate immune response and tissue homeostasis. Monocytes differentiate into unpolarized macrophages (M0) which are polarized into M1 (pro-inflammatory) or M2 (anti-inflammatory) macrophages depending on the stimuli. The effect of TRAIL on monocytes/macrophages is poorly understood.

In this study, the transcriptional effect of TRAIL signaling on the differentiation of primary human monocytes to M0 and M1 macrophages is investigated. Primary human monocytes were either treated or untreated during differentiation into macrophages then the cells were either polarized to M1 macrophages or kept as unpolarized. To uncover the transcriptional differences in the TRAIL-treated macrophage group, RNA-sequencing was employed and differentially expressed genes were validated by qPCR. In addition, the level of CXCL11 and TNF in the cell supernatant was analyzed by ELISA.

TRAIL stimulation during macrophage differentiation increased the expression of CXCL9 and TNF, whereas it decreased the expression of CXCL8 and CXCL5 in M0 macrophages. Moreover, the expression of HGF and PACERR was decreased in M1 macrophages, whilst both mRNA and protein levels of TNF and the protein level of CXCL11 were enhanced.

In summary, our results show that TRAIL-DR4/5 signaling activation during macrophage differentiation drives monocytes to differentiate into M1-like macrophages. Our study sheds new light on mechanisms of monocyte-to-macrophage differentiation by defining TRAIL as a new modulator.

Keywords: Monocytes, macrophages, TRAIL, death receptorsDR4/5

ÖLÜM RESEPTÖRÜ AKTİVASYONUNUN PRİMER İNSAN MONOSİTLERİNİN M1 MAKROFAJLARINA DÖNÜŞMESİNE ETKİSİNİN TRANSKRİPTOMİK ANALİZİ

Ayşenur Öner, Dokuz Eylül Üniversitesi, İzmir Uluslararası Biyotıp ve Genom Enstitüsü, Moleküler Biyoloji ve Genetik, İzmir/Türkiye

ÖZET

TNF ile ilişkili apoptoz indükleyici ligand (TRAIL), TNF ailesinin bir üyesidir ve apoptozu veya sağ kalım yolaklarını aktive eder. TRAIL'ın normal hücreleri etkilemeden kötü huylu hücrelerde apoptozu indükleme yeteneği, TRAIL'ın kanser tedavisinde kullanılmasının önünü açmıştır.

Makrofajlar hem inflamasyona yanıt verirler hem de doku homeostazının korunmasında rol oynarlar. Dolaşımdaki monositler dokuda makrofajlara (M0) dönüşürler ve bu makrofajlar uyaranlara bağlı olarak M1 (proinflamatuar) ya da M2 (antiinflamatuar) makrofajlara polarize olurlar. TRAIL'ın kanser üzerindeki etkisi bilindiği halde monositler/makrofajlar üzerindeki etkisi tam olarak aydınlatılmamıştır.

Bu çalışmada, TRAIL sinyalinin primer insan monositlerinin M0 ve M1 makrofajlarına farklılaşması üzerindeki transkripsiyonel etkisi araştırılmaktadır. İnsan primer monositlerinin bir kısmı yedi gün boyunca sadece M-CSF ile inkübe edilirken diğer kısım M-CSF ve TRAIL ile inkübe edilmiştir. Yedinci günün sonunda, makrofajların bir kısmı M1 makrofajlarına polarize edilirken bir kısmı da polarize edilmedi. TRAIL ile uyarılan makrofajların gen düzeyindeki ifade değişikliklerini incelemek için RNA dizilimi yöntemi kullanıldı. Bu analizin sonucunda değişiklik gösteren genlerin doğrulanması qPCR yöntemi ile yapıldı. CXCL11 ve TNF sitokinlerinin konsantrasyonu ELISA yöntemi ile ölçüldü.

Makrofaj farklılaşması sırasında TRAIL stimülasyonu, M0 makrofajlarında CXCL9 ve TNF ifadesini arttırırken, CXCL8 ve CXCL5 ifadesini azalttı. Bunun yanı sıra, M1 makrofajlarında HGF ve PACERR ifadesini azaltırken, TNF'nın mRNA ve protein seviyesini arttırmıştır. CXCL11'in gen ifadesinde düşüş gözlemlenirken protein seviyesi artmıştır.

Özetle, sonuçlarımız makrofaj farklılaşması sırasında TRAIL-DR4/5 sinyal aktivasyonunun monositleri M1 makrofajlarına farklılaşmaya yönlendirdiğini göstermektedir. Çalışmamız TRAIL'ı yeni bir modülatör olarak tanımlayarak monosit-makrofaj farklılaşma mekanizmasına yeni bir ışık tutmaktadır.

Anahtar Kelimeler: TRAIL, ölüm reseptörleri, monosit, makrofaj

1. INTRODUCTION AND GOALS

1.1. Definition and Importance of the Problem

Macrophages originate from circulating monocytes in the peripheral blood and are found in essentially every organ and tissue, comprising the first line of defense against any disease. They are schematically classified as M1 (classically activated) and M2 (alternatively activated) macrophages which are even further subdivided into M2a, M2b, M2c and M2d. M1 macrophages produce pro-inflammatory cytokines against pathogens leading to tissue damage, whereas M2 macrophages release anti-inflammatory cytokines to enhance tissue repair. M1/M2 balance plays a critical role in the development and progression of many diseases. For instance, the increased number of M1 macrophages is associated with type II diabetes, while increased number of M2 macrophages is associated with cancer. Therefore, uncovering the mechanisms associated with the modulation of macrophage phenotype in response to environmental stimuli holds immense clinical promise for many diseases.

TNF-related apoptosis-inducing ligand (TRAIL) that is a member of the TNF superfamily proteins induces apoptosis like other members of this superfamily, but only in malignant cells without harming normal cells. Despite the fact that TRAIL has been addressed as a promising anticancer therapeutic, little is known about noncanonical functions on normal cells, especially on immune cells. As a matter of fact, it has been shown that TRAIL signaling plays a physiological role in the maturation of monocytes and monocyte migration. However, the immunomodulatory effect of TRAIL on monocyte to macrophage differentiation has not been fully understood.

1.2. Research Objective

The first step was to determine the expression level of functional TRAIL receptors, DR4 and DR5, on monocyte subsets by flow cytometry. Afterwards, the susceptibility of monocytes/macrophages to recombinant human TRAIL-mediated apoptosis was tested by Annexin V/7AAD assay. Subsequently, RNA-sequencing (RNA-seq) was performed to investigate the transcriptional changes in macrophages treated with TRAIL during monocyte to macrophage differentiation. Next, a selected set of differentially expressed genes in TRAIL-treated macrophages and control macrophages were further validated by RT-qPCR. Finally, the impact of TRAIL during monocyte to macrophage differentiation on the pro-inflammatory cytokine release of macrophages was analyzed by ELISA.

1.3. Hypothesis

Treatment of primary human monocytes with TRAIL during monocyte to macrophage differentiation enhances the expression of pro-inflammatory markers while attenuating the expression of anti-inflammatory markers in monocyte-derived macrophages.

2. GENERAL INFORMATION

2.1. Immune System

The immune system is a network of various specialized cells, tissues, organs and proteins that function to distinguish self from non-self, thereby protecting the organism from numerous pathogens. Although the immune system has been basically depicted as a defense mechanism, the immune system participates an important role in a variety of physiological processes such as tissue homeostasis, development and wound healing (Rankin & Artis, 2018; Henson & Hume, 2006). This versatile system is composed of two facets, innate and adaptive immunity.

The innate immunity of the organism has strategies to deal with the threat posed by disease-causing microorganisms: anatomic (skin and mucous membrane) barrier and chemical (antimicrobial proteins) barrier (Marshall et al., 2018; Murphy & Weaver,2017). Once pathogens breach the barriers of the host, the cellular defenses of innate immunity provide a rapid response against invasion by pathogens. The cells in the innate immune system recognize pathogens via pattern recognition receptors (PRRs) which enable immune cells to identify and react to a range of pathogens that have common molecular components not found in the host system called pathogen-associated molecular patterns (PAMPs) (Tang et al., 2012; Medzhitov & Janeway, 2000). The innate immunity response is mediated by granulocytes (neutrophils, eosinophils, basophils and mast cells), monocytes/macrophages, natural killer cells (NKs), innate lymphoid cells (ILCs) and dendritic cells (Marshall et al., 2018; Gasteiger et al., 2017). Neutrophils, macrophages and dendritic cells detect the presence of microbial elements and initiate immune responses by either effector function such as phagocytosis or by producing inflammatory mediators, cytokines and chemokines, to recruit other immune cells, such as NK cells and ILCs (Murphy & Weaver, 2017). Upon activation of these cells, the main mechanisms to execute the target are the release of granules containing cytotoxic granzymes and perforin and also the secretion of mediators that have antiviral activity (Ramírez-Labrada et al., 2022; Murphy & Weaver, 2017). The clearance of invading pathogens by innate immunity can fail due to its primitive form of immunological memory and the narrow size of the antigen recognition repertoire (Netea et al., 2019; Farber et al., 2016; Vivier & Malissen, 2005). Hence, a more specific response is mounted by the adaptive immune system once the immune response of innate immunity is not sufficient (Abbott & Ustoyev, 2019).

The innate immune cells are responsible for the initiation and subsequent direction of adaptive immune responses to the site of inflammation. Macrophages and dendritic cells process the antigen of an invader and display for recognition by lymphocytes, T and B cells, to initiate an adaptive immune response (Gaudino & Kumar, 2019; Bonilla & Oettgen, 2010; Zhao et al., 2009). These innate immune cells, therefore, called antigen-presenting cells (APCs), serve as an essential link between the innate immune response and the adaptive immune response. The effective cellular and humoral adaptive immune response are accomplished via massive antibody production by B cells against antigens and elimination of the pathogens by cytotoxic T cells together with helper T cells (Abbott & Ustoyev, 2019). This unique feature of adaptive immunity is possible owing to the highly diverse development of a diverse repertoire of antigen receptors, allowing recognition of any potential threat (Netea et al., 2019; Vivier & Malissen, 2005). Even if the development of the precise response by adaptive immunity takes a few days or weeks, it is crucial for the generation of long-lived immunological memory that the ability of the adaptive immune system to stronger response against the antigen encountered previously in the event of re-expose (Netea et al., 2019; Netea et al., 2017).

2.2. Macrophages, the big eaters

2.2.1. The origin of macrophages

Macrophages that have been existed for more than 500 million years were discovered by Russian zoologist Ilya Ilyich Mechnikov at the end of the 19^{th} century (Poltavets et al., 2020). Macrophages are ubiquitous in all tissues of adult mammals, exhibiting a wide variety of morphological and physiological characteristics. In light of recent findings, two distinct populations of macrophages can be distinguished by their progenitors and developmental history (Perdiguero & Geissmann, 2016). The large population of the resident tissue macrophages arise during embryogenesis and have self-renewal capacity and the other large population is produced from a hematopoietic stem cell in the bone marrow (Wu & Hirschi, 2021; Epelman et al., 2014; Sieweke & Allen, 2013). Among the resident macrophages are the red pulp macrophages of the spleen, the alveolar macrophages of the lungs, the epidermal Langerhans cells, the brain microglia, the liver Kupffer cells, peritoneal macrophages, and the F4/80^{bright} macrophages of the pancreas, kidney and cardiac macrophages (Perdiguero & Geissmann, 2016).

Monocytes are derived from a common myeloid progenitor cell originating from hematopoietic stem cells in the bone marrow that also give rise to various leukocytes. Monocytes are a heterogeneous group of cells that are categorized into subsets upon the surface expression of CD14 and CD16 markers which are part of the lipopolysaccharide receptor and Fc receptor, respectively (Ziegler-Heitbrock, 2007). The most common type of monocyte subset in human blood is $CD14^{++}CD16^{-}$ monocytes are referred to as classical monocytes and the CD16+ monocyte population is divided into two subsets, $CD14^{+}CD16^{++}$ and $CD14^{++}CD16^{+}$ monocytes referred to as non-classical and intermediate monocytes, respectively (Ziegler-Heitbrock et al., 2010).

Once monocytes are released into the peripheral blood, circulating monocytes migrate to tissues affected by local growth factors, pro-inflammatory cytokines, and microbial elements during both homeostasis and inflammation (Shi & Pamer, 2011). CCL2 (also known as monocyte chemoattractant protein-1, MCP-1) presented by the endothelium is the most potent chemokine that promotes extravasation of $CD16^{-}$

monocytes to the site of inflammation (Gschwandtner et al., 2019; Ghousifam et al., 2019; Hardy et al., 2004). CX3C-chemokine ligand 1 (CX3CL1) and CXC-chemokine ligand 12 (CXCL12) initiated the migration of CD16+ monocytes due to low expression of CCR2 (Ancuta et al., 2003). The steps of monocyte extravasation are capture, slow rolling on the endothelium, firm adhesion/arrest, intraluminal crawling, and transmigration (Gerhardt & Ley, 2015). Monocyte colony-stimulation factor (CSF-1 or M-CSF) produced in the tissue is the primary growth factor for survival, proliferation and differentiation of maturation of blood monocytes (Sauter et al., 2016; Korkosz et al., 2012; Pixley & Stanley, 2004).

2.2.2. The populations of macrophages

Since the discovery of macrophages, macrophages have been depicted as a key element of the innate immune system due to their specialized scavenger, pattern-recognition and phagocytic receptors to sense and respond to tissue invasion by pathogens (Zagórska et al., 2014; Canton et al., 2013; Gautier et al., 2012; Kawai & Akira, 2010). In addition, macrophages maintain vital homeostatic roles, such as clearance of $2x10^{11}$ erythrocytes each day, removal of cell debris, clearance of lipoproteins and recycling iron, bilirubin and calcium for the host to reuse (Mosser et al., 2021; Biswas & Mantovani, 2012; Kohyama et al., 2009).

The hallmark of macrophages is their plasticity which enables them to change their physiology and phenotype and respond to environmental signals. Unpolarized macrophages (M0) respond to signaling molecules produced by active lymphocytes (T helper 1 or T helper 2) or wounded tissue (Mauro et al., 2016). Therefore, the nature of cytokines found in the environment, M0 macrophages are typically polarized into proinflammatory (M1) and anti-inflammatory (M2) macrophages (Yao et al., 2019; Li et al., 2018) (**Figure 1**). "Macrophage polarization" is the term utilized to describe this phenomenon of the different M1/M2 phenotypes. These extreme M0 phenotypes (M1 and M2) are widely investigated *in vitro*, notwithstanding the fact that M0 activation *in vivo* represents a continuum of functional phenotypes with intermediate or overlapping characteristics (Bozec & Soulat, 2017).

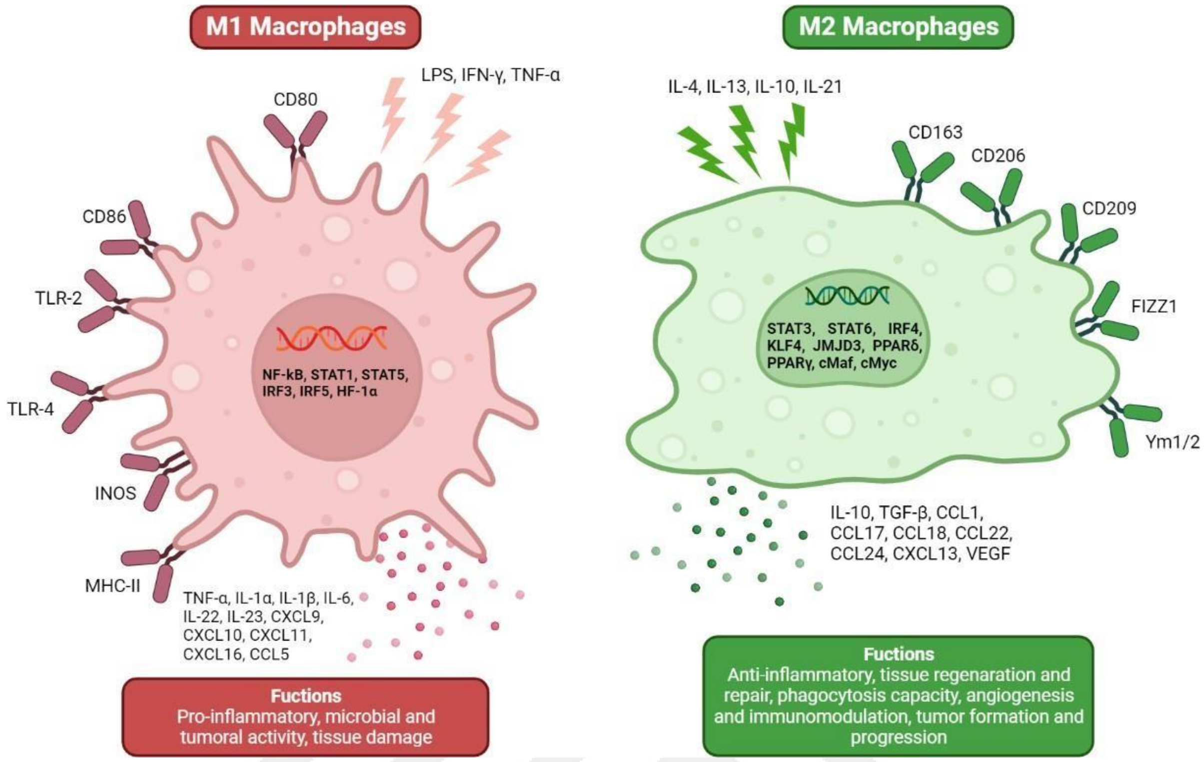

Figure 1. The summary of different stimuli, surface markers, cytokines and biological functions conducted by M1 and M2 macrophages.
CCL, chemokine (C-C motif) ligand; cMaf, c-musculoaponeurotic fibrosarcoma; CXCL, chemokine (C-X-C) ligand; FIZZ1, resistin-like α; HIF, hypoxia-inducible factor; iNOS, inducible nitric oxide synthase; IFN-γ, interferon-gamma; IL, interleukin; IRF, interferon regulatory factor; JMJD, Jumonji domain-containing protein; KLF, Kruppel-like factor; NF-κB, nuclear factor κB; KLF, Kruppel-like factor; LPS, lipopolysaccharides; MHC, major histocompatibility complex; PPAR, peroxisome proliferator-activated receptors; STAT, signal transducer and activator of transcription; TLR, Toll-like receptor; TNF, tumor necrosis factor alpha; TGF-β, transforming growth factor beta; VEGF, vascular endothelial growth factor; Ym1, chitinase 3-like 3. *Created with BioRender.com*

M1 macrophages are also known as classically activated cells referred to designate the effector macrophages that participate in the cell-mediated immune response. Toll-like receptor (TLR) ligands, such as LPS or IFN-γ produced by Th1 cells polarized macrophages to M1 macrophages and prime them to secrete pro-inflammatory cytokines such IL-23, IL-12, IL-6 and tumor necrosis factor (TNF) (de Gaetano et al., 2016; Abumaree et al., 2013; Barros et al., 2013). The high expression of TLR-2, TLR-4, CD80, CD86, iNOS, and MHC-II surface phenotypes are characteristics of M1 macrophages that also produce a variety of cytokines and chemokines (such as TNF, IL-1, IL-1, IL-6, IL-12, CXCL9, and CXCL10) that have a stimulating effect on unpolarized macrophages (Murray, 2017). It has been demonstrated that master transcription factors like NF-kB, STAT1, STAT5, IRF3, and IRF5 regulate the expression of M1 genes (Zhou et al., 2014). These classically activated macrophages have a central role in host defense, inducing cytotoxic activity against pathogens and malignant cells, but it's critical to keep their activation under strict control because the cytokines and mediators they secrete can harm the tissues of the host (Wang et al., 2014; Martinez & Gordon, 2014).

Similar to M1 macrophages, M2 macrophages can develop in response to innate or adaptive stimuli. Alternatively, activated macrophages can be further categorized into the subtypes M2a, M2b, M2c, and M2d (**Figure 2**). Upon stimulation with IL-4/IL-13 and downstream involvement of jumonji domain-containing-3 (Jmjd3) and interferon regulatory factor (IRF)-4, nonpolarized macrophages are polarized into M2a macrophages (Satoh et al., 2010). Immunoglobulin complexes in combinati on with TLR agonists induced M2b macrophage phenotype while IL-10, transforming growth factor (TGF), or glucocorticoids induce M2c macrophage phenotype (Porta et al., 2015). Lastly, the fourth phenotype of M2 macrophages, M2d macrophages are induced by TLR ligands and A2 adenosine receptor(A2R) agonists or by IL-6 and they release IL-10 and TGF-ß and VEGF in a high-level and low expression of TNF and IL-12 ((Wang et al., 2010; Duluc et al., 2007). Additionally, the expression of surface markers such as the mannitol receptor, CD206, CD163, CD209, FIZZ1, and Ym1/2 can help identify M2 macrophages (Liao et al., 2011). Unpolarized macrophages are drawn to polarize into the M2 phenotype by up-regulation of cytokines and chemokines like IL-10, TGF-ß, CCL1, CCL17, CCL18, CCL22, and CCL24 and it has been demonstrated that key transcription factors, including STAT6, IRF4, JMJD3, and PPAR modulate the expression of M2 genes (Wang et al., 2014; Mulder et al., 2014; Gordon & Martinez, 2010). The main contributions of M2 macrophages are immunomodulation, tissue repairing, angiogenesis, and aid in the resolution of inflammation(Viola et al., 2019; Ferrante et al., 2013).

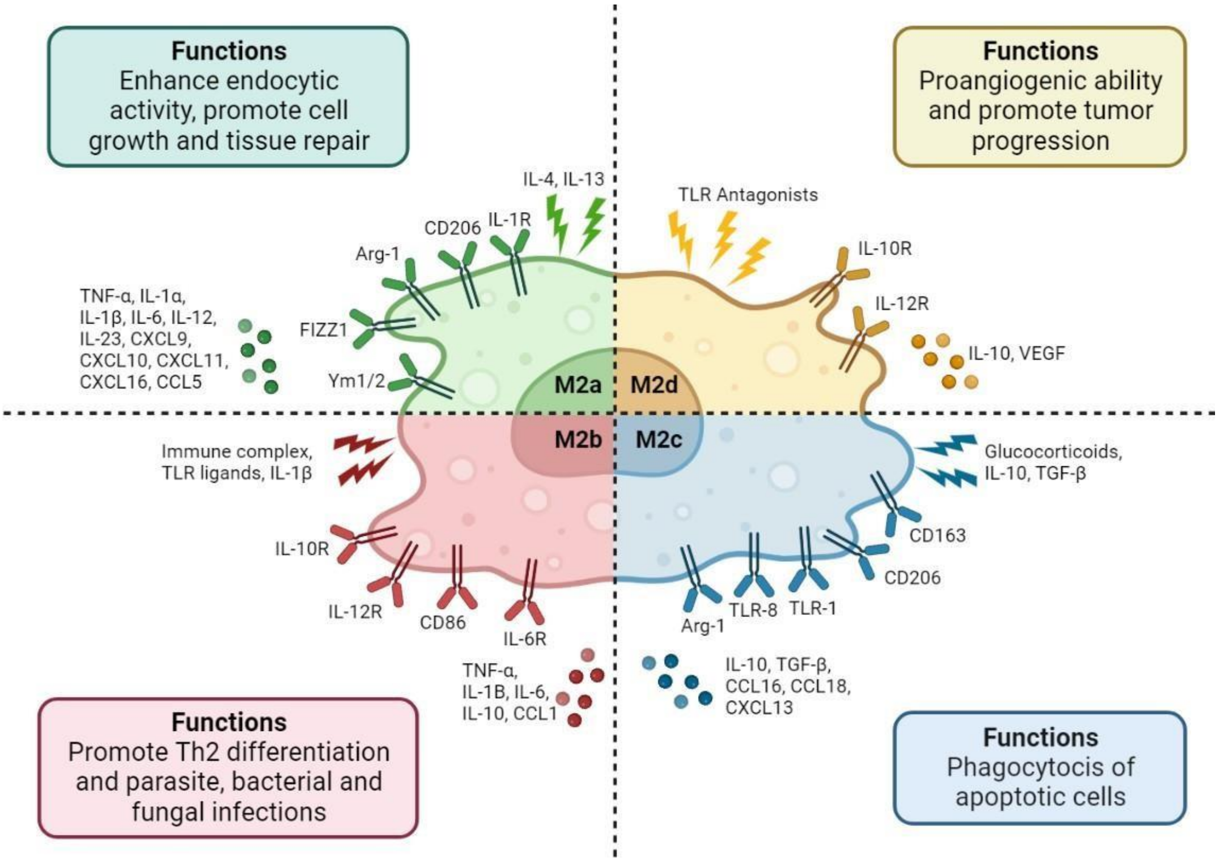

Figure 2. The summary of different stimuli, surface markers, cytokines and biological functions conducted by M2 subsets.

Created with BioRender.com

2.2.3. Macrophages in diseases

Multiple organs and tissues are affected by a variety of disorders known as autoimmune diseases. Uncontrolled or excessively inflammatory immune responses are thought to be important disease drivers and contributors, despite the fact that the causes of many autoimmune diseases remain unknown. Many chronic inflammatory diseases and autoimmune disorders, such as rheumatoid arthritis (RA), experimental autoimmune encephalomyelitis (EAE), multiple sclerosis (MS), autoimmune hepatitis, Crohn's disease, and inflammatory bowel disease (IBD), are largely associated with an altered balance of M1/M2 macrophage phenotypes (Jiang et al., 2014; Wynn et al., 2013).

Inflammatory bowel disease(IBD) is characterized by a chronic inflammatory condition in the small or large intestine that M1 macrophages produce pro-inflammatory cytokines such as IL-12, and TNF together with reactive metabolites worsen the disease condition (Miyanaka et al., 2007; Suzuki et al., 2001). Similar to IBD disease, M1 macrophages promote rheumatoid arthritis progression by releasing various inflammatory cytokines such as IL-23, and TNF, leading to the development of chronic polyarthritis (Gordon et al., 2012). M1 macrophages have also been implicated in inducing axonal loss in multiple sclerosis and experimental autoimmune encephalomyelitis by recruiting T cells which contribute to disease development and severity (Jiang et al., 2014; Perry et al., 2010). Another example of chronic inflammation mediated by M1 macrophages is type-2 diabetes originating from obesity which is characterized by impaired insulin secretion from pancreatic beta cells. M1 macrophages play an important role in the development of insulin resistance and pancreatic beta cell dysfunction upon production of TNF, iNOS, IL-1ß (Weisberg et al., 2003).

There are also pathologies correlated with increased activity of M2 macrophages, predominantly in asthma and allergic disorder. Macrophages located in the lung environment of asthmatic patients drive their polarization toward the M2 phenotype via type-2-associated cytokines including IL-4, IL-13 and IL-33 (Locksley, 2010). The presence of M2 macrophages together with these cytokines creates a synergistic effect, resulting in the recruitment of eosinophils, basophils and T_H2 cells that worsens disease symptoms (Kurowska-Stolarska et al., 2009; Sica and Mantovani, 2012).

2.2.4. Macrophages in cancer

The tumor microenvironment (TME) is abundantly populated by tissue-resident macrophages and recruited macrophages. Macrophages phenotypically polarize to a spectrum of activation states in response to tumor-derived or microenvironmental signals and these macrophages are called tumor-associated macrophages (TAMs) (Mantovani et al., 2008). TAMs can enhance tumor angiogenesis, promote tumor cell proliferation, invasion, and metastasis, and suppress the antitumor immune response mediated by T cells, resulting in promoting tumor growth and metastasis. Since the absence of M1-orienting signals and abundant level of M2 polarization factors produced by T_H2 lymphocytes and stromal cells in the TME, TAMs resemble the M2 macrophage phenotype (Liu et al., 2021; Zhou et al., 2017).

A variety of cytokines including epithelial growth factor (EGF), platelet-derived growth factor (PDGF), TGF-b1, hepatocyte growth factor (HGF), and epithelial growth ligands of the factor receptor (EGFR) family and basic fibroblast growth factor (BFGF) expressed by TAMs play an important role in tumorigenesis and tumor survival (Yin et al., 2016). TAMs exert a direct effect on promoting metastasis via secreting matrix metalloproteinases (MMPs) and also a group of angiogenic molecules such as VEGF, PDGF, and TGF-ß, supporting blood vessel formation (Hao et al., 2017). In addition to these functions, TAM-derived factors suppress cytotoxic T-cell response and NK-cell response (Dongre & Weinberg, 2019). The suppression of $CD8^+$ T cells is partly dependent on the presence of reactive oxygen species and IL-10 produced by TAMs and partly on the presence of T_{reg} in the tumor environment (Lu et al., 2011).

As it was outlined in the previous paragraph, since an increased number of TAM in TME associated with low survival rates in many human cancers, TAMs become potential biomarkers for the diagnosis of cancer and novel target for the treatment of cancers including decreasing blood monocytes recruitment, targeting TAMs activation, reprogramming TAMs to anti-tumor phenotype and targeting TAM-specific markers (Pan et al., 2020). As the plasticity of macrophages is their key characteristic, reprogramming M2-like TAMs to M1 macrophages that have antitumor macrophages is a promising treatment strategy.

M1/M2 balance plays a critical role in the development and progression of many diseases including human cancers. Therefore, it will be critical to obtain a better understanding of the M1/M2 balance to develop promising strategies and therapeutic agents for disease treatment. Reprogramming macrophage phenotype has shown remarkable advancements in recent ongoing experimental, preclinical, and clinical research.

2.3. Tumor necrosis factor (TNF)-related apoptosis-inducing ligand (TRAIL)

TNF-related apoptosis-inducing ligand (also known as Apo-2L) is a type II transmembrane that is a member of the TNF family proteins based on its homology on its C-terminal extracellular part with Fas ligand and TNF (Pitti et al., 1996; Wiley et al., 1995). Unlike other members of the TNF family, TRAIL induces apoptosis in malignant and infected cells without harming normal cells through oligomerization with its death receptors, DR4(TRAIL-R1) and DR5(TRAIL-R2) (LeBlanc & Ashkenazi, 2003; Ashkenazi et al., 1999). There are two forms of TRAIL ligand that are membrane-bound form and soluble form which is proteolytically cleaved from the cell surface. The human TRAIL interacts with four membrane death receptors and one soluble receptor that DR4 and DR5 and induces apoptosis via a conserved cytoplasmic death domain involved in caspase activation. The other two membrane receptors TRAIL-R3 (DcR1) and TRAIL-R4(DcR2) do not induce apoptotic signals due to the absence of a death domain on their structure which therefore are considered to act as decoy receptors. The soluble TRAIL receptor family member is osteoprotegerin (OPG) which binds to TRAIL with lower affinity and its physiological role as a consequence of this interaction remains elusive. Although there is a recent study suggesting that tumor-derived OPG attenuates the apoptosis activity of TRAIL in prostate cancer cells (Holen et al., 2002).

2.3.1. TRAIL canonical signaling

Upon TRAIL binding to its functional receptors, DR4 or DR5, specific cytoplasmic proteins recruits to the intracellular death domain of the receptor, forming a death-inducing signaling complex (DISC) (Bodmer et al., 2000) (**Figure 3**). Apoptosis-initiating procaspase-8 and/or procaspase-10 are recruited to the DICS by Fas-associated death domain (FADD) adaptor protein (Sprick et al., 2002; Kischkel et al., 2001). Thereafter, initiator caspases, caspase-8 and caspase-10, are activated and the subsequent release of their active cleaved forms to the cytosol where transduce the signal to the apoptotic executioner caspases such as caspase-3, caspase-6 and caspase-7 (Wang et al., 2001). Once executioner caspases cleave vital cellular proteins, the molecular process of apoptosis began. This type of apoptosis initiated externally via death ligands is referred to as the extrinsic apoptosis pathway. Although extinctic pathways are sufficient to induce apoptosis in a certain type of cells, some cells require amplification of the apoptosis signal via the mitochondrial apoptotic pathway, known as the intrinsic apoptosis pathway (Ozören & El-Deiry, 2002; Scaffidi et al., 1998). To activate the intrinsic apoptosis pathway, caspase-8 firstly cleaves the anti-apoptotic Bcl-2 inferring pro-apoptotic proteins then tBid translocated to the mitochondria to enhance the release of cytochrome c by other pro-apoptotic proteins, resulting in the initiation of apoptosis via effector caspases cleaved by apoptosome (Li et al., 1998; Scaffidi et al., 1998).

2.3.2. TRAIL non-canonical signaling

Apart from inducing apoptosis, TRAIL initiates noncanonical signaling through the activation of proinflammatory pathways, such as PI3K/Akt (phosphoinositide 3-kinases /protein kinase B), Nf-kB (factor nuclear kappa B), MAPK (mitogen-activated protein kinase), JNK (c-Jun N-terminal kinase), ERK (extracellular signal-regulated kinase), and p38 (Morel et al., 2005; Lin et al., 2000; Franco et al., 2001; Degli-Esposti et al., 1997; Chaudhary et al., 1997). Intriguingly, more recent evidence shows that TRAIL participates in apoptosis-independent effects in normal cells including proliferation, migration, differentiation and inflammation. The proliferation of fibroblasts isolated from synovial tissue, vascular smooth muscle cells (VSMCs), primary human endothelial cells, and proximal tubular epithelial cells, for instance, has been demonstrated to be induced by TRAIL, activating the NF-kB, ERK1/2, p38, and PI3K-AKT pathways (Chan et al., 2010; Secchiero et al., 2004). Additionally, TRAIL induces the ERK1/2 pathway, which facilitates VSMC migration, and it causes human endothelial cells to produce NF-kB and inflammatory genes (Kavurma et al., 2008; Secchiero et al., 2003).

A)

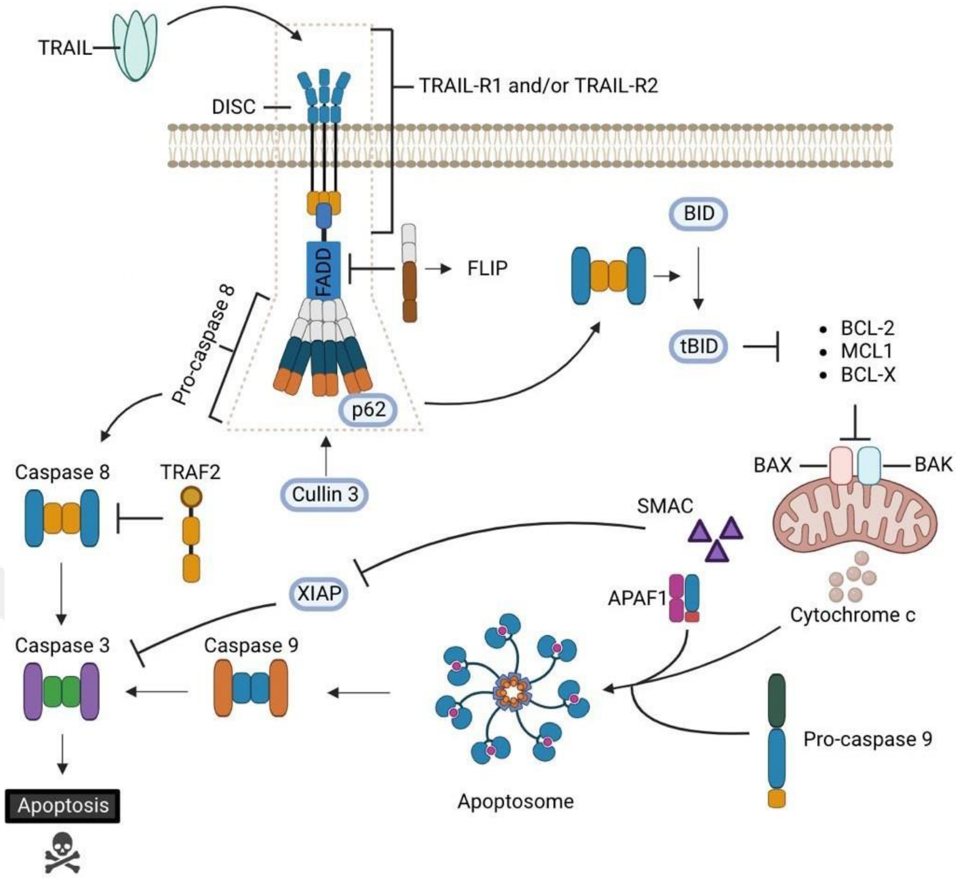
TRAIL
DISC
TRAIL-R1 and/or TRAIL-R2
FADD
FLIP
Pro-caspase 8
p62
BID
tBID
BCL-2
MCL1
BCL-X
BAX
BAK
Cullin 3
Caspase 8
TRAF2
SMAC
XIAP
APAF1
Cytochrome c
Caspase 3
Caspase 9
Pro-caspase 9
Apoptosome
Apoptosis

B)

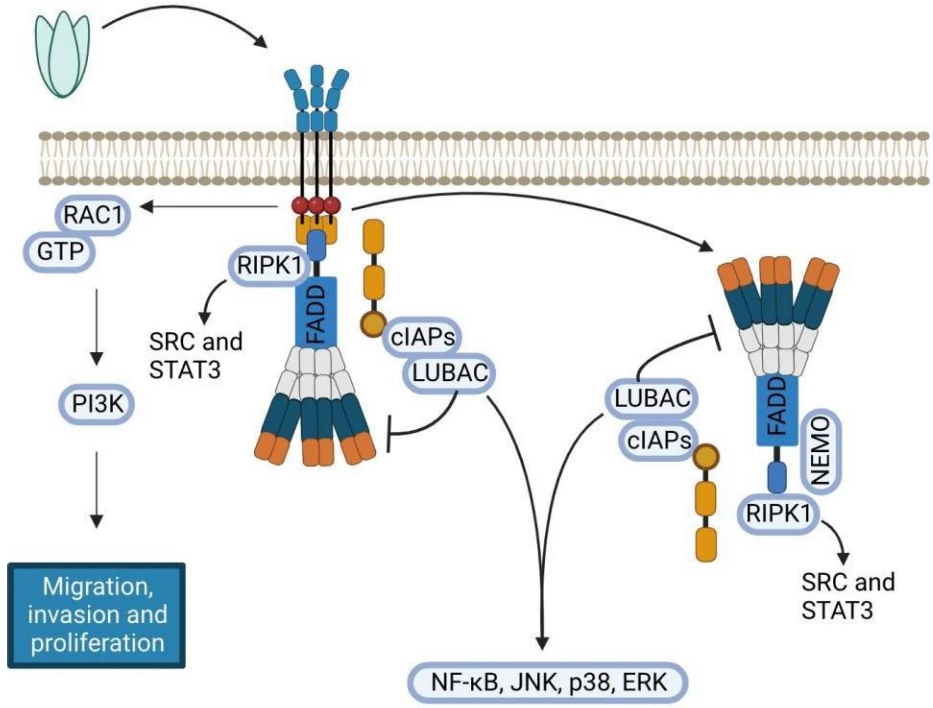
RAC1
GTP
RIPK1
FADD
SRC and
STAT3
cIAPs
LUBAC
PI3K
LUBAC
cIAPs
FADD
NEMO
RIPK1
SRC and
STAT3
Migration,
invasion and
proliferation
NF-κB, JNK, p38, ERK

Figure 3. TRAIL-mediated signaling pathways.

A) Canonical pathway of TRAIL signaling that initiates apoptosis via a caspase-dependent pathway. **B)** Non-canonical TRAIL signaling that participate in distinct cellular process within the cell. *Created with BioRender.com*

2.3.3. The anti-apoptotic effect of TRAIL

A widely held consensus is that the majority of studies on TRAIL focused on its clinical applications for cancer, but the immunomodulatory functions of TRAIL on immune cells are still not fully understood as both TRAIL and immune cells are vital players in both inflammation and anti-tumor response. TRAIL signaling is particularly important for the resolution phase of an immune response, especially effector cell removal which prevents autoimmune disorders. Blocking TRAIL exacerbated the disease in various rheumatoid arthritis (RA) mice models. In these RA models, TRAIL had little impact on the death of inflammatory cells, but it did impede lymphocyte cell cycle progression, restrain T-cell proliferation, and decrease cytokine production (Chyuan et al., 2018; Song et al., 2000). Additionally, experimental autoimmune encephalomyelitis (EAE) in mice was made worse by inhibiting TRAIL signaling (Hilliard et al., 2001). However, other studies showed that TRAIL promotes granzyme B production in NK cells, and also TRAIL signaling promotes $CD4^+$ T cell function and expansion (Cardoso Alves et al., 2020; Ikeda et al., 2010). These findings imply that TRAIL might have a different function in the context of physiological conditions and cell types. In spite of macrophages being the most important immune cells in tissue homeostasis and inflammation, the immunomodulatory function of TRAIL in macrophages is poorly understood.

2.3.4. Immunomodulatory function of TRAIL on monocytes and macrophages

Specifically, in monocytes and macrophages, TRAIL signaling has been shown to participate in different cellular processes, including maturation, migration, and pro-inflammatory cytokine production. TRAIL signaling promotes monocytic maturation of HL-60 cells in the absence of cytotoxicity strongly suggesting that this is a demonstration of a positive regulative effect of TRAIL on monocytic cell line in a caspase-dependent manner (Secchiero et al., 2002). Furthermore, TRAIL acts as a chemotactic factor for TRAIL-treated THP-1 cells and LPS-primed primary human monocytes which is mediated by DR4 via Rho GTPase and its downstream effectors (Wei et al., 2010). Another finding of the immune regulatory mechanism of TRAIL on macrophages is that TRAIL promotes cytokine secretion such as IL-1ß and TNF by macrophages via NF-kB activation after ischemia/reperfusion injury and researchers hypothesize that TRAIL play role in macrophage polarization into M1 phenotype as pro-inflammatory cytokine production increases in the presence of TRAIL (Jiang et al., 2017). Accordingly, in a study, TRAIL enhanced the production of IL-1ß, IL-6, and TNF in TAMs of both humans and mice, implying that TRAIL might aid in re-educating TAMs to adopt proinflammatory phenotype (Gao et al., 2015).

As outlined in previous paragraphs, although *in vitro* tumor studies have significantly advanced our understanding of TRAIL signaling, it is still challenging to explain the complex dynamics of immunoregulation in TRAIL-mediated macrophages and these results offer a valuable background for further studies to understand the physiological functions of TRAIL on macrophage re-education.

3. MATERIALS AND METHODS

3.1. Type of Research

This study was carried out under *in vitro* conditions.

3.2. Date and Location of Research

The part of the study up to the RNA-sequencing was performed at Sag Lab. in Izmir Biomedicine and Genome Center, from March 2021 to December 2021. The qPCR validation experiments were started at Cell Stress Discoveries Center, Galway/Ireland from November 2021 to May 2022. The experiments were finished at Sag Lab in Izmir Biomedicine and Genome Center, from June 2022 to September 2022.

3.3. Universe and Sample of Research/Research Groups

Primary human monocytes and monocyte-derived macrophages were used for this study and primary human monocytes were collected from buffy coats of healthy donors at the age of 20-40.

3.4. Research Materials

3.4.1. General laboratory equipment

Table 1. The list of general laboratory instruments used in the experiments

Equipment Type	Manufacturers and Brands of Instruments
Cell Analyzer	BD Biosciences, LSRFortessa, FACSCanto™ II
Centrifuge	Eppendorf, 5702 and 5415R
CO_2 Incubator	Memmert, INCO153 and Eppendorf, CellXpert
Freezer(-20 ^{0}C)	Bosch, KSV 36 A 131
Refrigerator (+4 ^{0}C)	Bosch, KSV 36 A 131
Freezer(-80 ^{0}C)	ThermoFisher Scientific, Forma 700 series and New Brunswick, U725-C
Ice Maker	Hoshizaki FM300 and Telstar, IF series

Inverted Microscope	Carl Zeiss, Axio Vert.A1 and Olympus, CKX41
Laminar Flow Cabinet	ThermoFisher Scientific, Thermo Safe 2020 and Telstar, Bio II Advance
Microcentrifuge	ThermoFisher Scientific, Thermo Micro CL 17R and Eppendorf, 5417C
Mini Spin Centrifuge	ThermoFisher Scientific, MYSPIN 6 and Eppendorf, Mini Spin Plus
Spectrophotometer	ThermoFisher Scientific, Nanodrop 2000
Pipette	Eppendorf :0,5-10µl, 2-20µl, 10-100µl, 20-200µl, 100-1000µl
RT-PCR	Applied Biosystems™, StepOnePlus™ and 7500 Fast Real-Time PCR System
Fine balance	Sartorius
Vortex	ThermoFisher Scientific, LP and Fisher Scientific
Water bath	Lauda, aquiline AL-12
Rocker	ThermoFisher Scientific, Compact Digital Rocker
Fume Hood	Mod Bus 2200 Airflow Monitor
Multichannel Pipette	200 µl Rainin
Microplate Reader	Thermo, Varioscan Flash

3.4.2. Chemicals, reagents and commercial kits

Table 2. The list of chemicals, reagents, ligands and commercial kits used in the experiments

Chemicals	**Catalog Number**	**Manufacturer**
2-mercaptoethanol (2ME)	M6250-250ML	Sigma-Aldrich
Reagents	**Catalog Number**	**Manufacturer**
1X Hanks' Balanced Salt Solution (HBSS), w/o Ca+2, w/o Mg+2	H9394-500ML	Sigma-Aldrich
RT-qPCR Brilliant III Probe Master Mix	600884	Agilent Technologies
Fetal Bovine Serum	10500-064	Gibco
Ficoll Paque PLUS	17144003	Sigma-Aldrich
Penicillin(10.000U/ml) /Streptomycin (10.000mg/ml)	15140122	ThermoFisher Scientific
Percoll PLUS	17544501	Sigma-Aldrich
RPMI 1640, w/o Phenol red, with 2.0 g/l NaHCO3, w/o L-Glutamine	E0500-350	Cegrogen
RPMI 1640, with 2.0 g/l NaHCO3, with L-Glutamine	11875093	Gibco,ThermoFisher Scientific
1X Phosphate Buffered Saline, w/o Ca^{+2}, w/o Mg^{+2}	10010-015	Gibco, ThermoFisher Scientific
10X Phosphate Buffered Saline, w/o Ca^{+2}, w/o Mg^{+2}	70011044	Gibco, ThermoFisher Scientific
Trypan Blue (0.4%)	BI03-102-1B	Biological Industries

FastStart Essential DNA Probes Master	6924492001	Roche Life Science
Ligands	**Catalog Number**	**Manufacturer**
Recombinant Human TRAIL	375-TL-010	R&D Systems
Recombinant Human IFN-γ	285-IF/CF	R&D Systems
Recombinant Human M-CSF	300-25	Peprotech
Ultrapure LPS	tlrl-3pelps	Sigma
Commercial Kits	**Catalog Number**	**Manufacturer**
RNeasy Mini Kit	74104	QIAGEN
QIAshredder	79654	QIAGEN
SuperScript™ IV First-Strand Synthesis System	18091050	Invitrogen
EvoScript Universal cDNA Master kit	7912455001	Roche Life Science
Monarch Total RNA Miniprep Kit	T2010S	New England BioLabs Inc.
PE Annexin V Apoptosis Detection Kit with 7-AAD	640934	BioLegend
Zombie UV Live/Dead Staining Kit	423108	BioLegend
Human TruStain FcX	422301	BioLegend
RNA 6000 Nano Assay Reagent Kit	5067-1511	Agilent Technologies

3.4.3. Consumables

Table 3. The list of consumables used for the experiments

Consumables	Manufacturer
0,2 ml PCR Tube	Axygen
0,5 ml PCR Tube	Sarstedt
1,5 ml Tube	Greiner
2 ml Tube	Greiner
5 ml FACS Tubes	Corning
Disposable serological pipette: 5,10 and 25 ml	Greiner
Filter Pipette Tips: 10, 200, and 1000 µl	Sarstedt and Neptune
Hemocytometer	Sigma-Aldrich
96-well PCR plate	Applied Biosystems
Pipette Tips: 10, 200, and 1000 µl	Vertex
Tissue Culture Plates: 6, 12, 24, 48, and 96 well	Greiner
Ultra-Low Attachment 6 well plates	Corning
Conical tubes: 15 and 50 mL	Sarstedt

3.4.4. qPCR primers

Table 4. The list of qPCR primer-probe assays used in qPCR experiments

Experimental Group	Gene Symbol	Catalog Number
M1 and TRAIL-treated M1	LILRA5	Hs.PT.58.39438843
	CXCL11	Hs.PT.58.26723814
	HGF	Hs.PT.58.81779
	PACERR	ACC# NR_125801.1 Set 1
M0 and TRAIL-treated M0	CXCL9	Hs.PT.58.27316119
	CXCL8	Hs.PT.58.38869678.g
	CXCL5	Hs.PT.58.41058007.g
	TNF	Hs.PT.58.45380900
Housekeeping Gene	HPRT1	Hs.PT.58v.45621572

3.4.5. Flow cytometry reagents

Table 5. The antibodies and reagents used for flow cytometry analysis

Markers	Conjugate	Clone	Origin	Isotype	Manufacturer
DR4	APC	DJR1	Mouse	IgG1, κ	BioLegend
DR5	PE	DJR2-4	Mouse	IgG1, κ	BioLegend
CD14	BV510	M5E2	Mouse	IgG2a, κ	BioLegend
CD16	PE Dazzle 594	3G8	Mouse	IgG1, κ	BioLegend

3.4.6. Common Media, Buffers, and Stock Solutions

Table 6. The components of the solutions prepared for the experiments

Solution	**The content of the solution**	**Storage Location**
Complete RPMI 1640 medium	RPMI 1640 with 1% Penicillin-Streptomycin, 1% L-glutamine, and heat-inactivated 5% FBS	+4°C
Percoll Solution	42.32% Percoll, 3.68% 10X PBS, 54.00% Complete RPMI 1640	Immediate usage
FACS Buffer	1X PBS with 1% BSA and 0,1 % sodium azide	+4°C
RNA Lysis Buffer (RNeasy Mini Kit)	RLT Buffer with %10 β-mercaptoethanol (β-ME)	RT
Ficoll Solution	Ficoll PM400 and sodium diatrizoate with calcium disodium ethylenediamine-tetra acetic acid	Immediate usage

3.4.7. ELISA kits

Table 7. The commercial kits for the ELISA procedure

Markers	**Catalog Number**	**Brand**
TNF	#430204	BioLegend
Human CXCL11/I-TAC	#DY672	R&D Systems

3.5. Variables of Research

Independent variables of the study: the presence or absence of TRAIL and M1 polarization factors.

Dependent variables of the study: the expression of death receptors(DR4/DR5), the expression levels of genes to be investigated, and the presence of dead cells.

3.6. Data Collection Methods

3.6.1. Primary human monocyte-derived macrophage generation

3.6.1.1. Isolation of human peripheral mononuclear cells(PBMCs) from buffy coat of healthy donors

Approximately 12 mL of buffy coat from healthy donors were transferred to a 50-mL conical tube. Blood samples were diluted 1:1 ratio with 1X PBS up to 20 mL. 15 mL Ficoll Paque PLUS solution was added into 50 mL conical tubes as much as the number of donors. Diluted samples of each donor were underlaid with Ficoll solution in related tubes. Then, the samples were centrifugated at 400 rcf for 35 minutes at RT without the break. PBMCs layered over the ficoll solution in the tubes were carefully harvested with a plastic Pasteur pipette into new 50-mL tubes containing complete RPMI 1640 (w/Phenol red) medium supplemented with heat-inactivated 5% FBS, 1% penicillin-streptomycin and 1% L-glutamine. Harvested PBMCs were washed twice with 1X PBS at 400 rcf for 10 minutes at RT. Afterwards, each donor's pellet of PBMCs was resuspended with 15 mL complete RPMI 1640 (w/o Phenol Red) medium

3.6.1.2. Isolation of primary human monocytes from PBMCSs from each donor

23.13 mL of Percoll PLUS was diluted with 1.87 mL of 10X PBS and inverted a few times to make a homogeneous solution and 2 mL was discarded from the solution. 23 mL of Percoll dilution were mixed with 27 mL complete RPMI 1640 (with Phenol Red) medium. For each donor, 25 mL of Percoll solution was carefully transferred to a 50 mL conical tube following PBMCs were slowly layered over Percoll solution in each related tube. The samples were centrifugated at 550 rcf for 35 minutes without break at RT. Monocytes accumulated in Percoll solution as a white cloudy phase were harvested with a plastic Pasteur pipette and transferred to a 50 mL tube containing about 5 mL of complete RPMI 1640 medium. Harvested monocytes were washed twice with 1X PBS at 400 rcf for 10 minutes at RT.

Monocytes of each donor were suspended into 5 or 10 mL complete RPMI 1640 medium according to the pellet size of monocytes and pipetting well to make homogeneous distribution of cells. 10 µl of monocytes of each donor were mixed with 10 µl trypan blue then to count cells using a hemocytometer, 10 µl cell suspension was added between the hemocytometer and cover glass via pipette. Cells were counted under an inverted phase-contrast microscope. For each donor sample, the total number of cells in four outer squares was counted and divided by four and the number is multiplied by 10^4 and the dilution factor. For one donor, normally 20 million up to 150 million monocytes were isolated.

3.6.1.3. Differentiation of human primary monocytes to macrophages

Freshly isolated monocytes of each donor were divided into two groups, the control group and the TRAIL-treated group. The control group was seeded as $1x10^6$ cells per mL in complete RPMI 1640 containing 10 ng/mL macrophage colony-stimulating factor (M-CSF) while the TRAIL-treated group was seeded as $1x10^6$ cells per mL in complete RPMI 1640 medium supplemented both 10 ng/mL M-CSF and 200 ng/mL recombinant human TRAIL protein. Totally, monocytes for each donor were plated in ultra-low attachment 6-well plates at a density of $3.5x10^6$ cells in 3.5 mL. Cells were incubated for 7 days in a 5% CO_2 incubator at +37°C for the fully differentiation of monocytes to macrophages.

On day three, the media replenished with 3.5 mL complete RPMI 1640 medium supplemented with both 10 ng/mL of M-CSF for control groups and with complete RPMI 1640 medium supplemented with both 10 ng/mL M-CSF and 200 ng/mL rhTRAIL for TRAIL-treated groups. When 7 days are up, macrophages were harvested by rinsing the wells with cold 1X PBS. Macrophages of each donor were collected in related 50 mL conical tubes and were centrifugated at 400 rcf for 5 minutes at room temperature. Macrophages of each donor were washed twice with warm-like 1X PBS with the same centrifugate configuration. In the last step, the macrophages of each donor were suspended in a complete RPMI 1640 medium.

3.6.1.4. Human primary monocytes-derived macrophages seeding and polarization

To attain the number of macrophages, 10 µl of cell suspension was mixed with 10 µl trypan blue and mixed well. 10 µl of the mixture was loaded onto a hemacytometer and cells were counted under an inverted light microscope. The total cell number of each donor was calculated.

Approximately 550.000 cells from each group of each donor were suspended in 1 mL of complete RPMI 1640 medium and were seeded into 24 well plates. Macrophages were incubated in a 37 °C cell culture incubator with 5% CO2 and 95% air overnight.

The next day, the supernatant of the cells was discarded and M1 macrophages of each donor were stimulated with complete RPMI 1640 supplemented with 100 ng/mL LPS and 20 ng/mL IFN-γ for 5 hours at the final volume of 500 µl. M0 macrophages remained as unpolarized. After 5 hours, the medium of M1 and M0 macrophages was transferred into 48 well plates for ELISA assay. Each well-containing experimental group was rinsed twice with warm-like 1X PBS and prepared for further analysis.

3.6.2. RNA Isolation

Total RNA was isolated from three biological replicates. After the macrophage polarization step, lysis buffer was added to each well. Cell lysate of each sample was transferred to related microcentrifuge tubes and placed on ice.

Cell lysate of each sample was transferred to a silica column and RNA binds to the silica while the rest of the other unnecessary constituents were washed out using a wash buffer including genomic DNA. In the last step, total RNA was eluted with 40 µl elution buffer from the silica beads via rehydrated with aqueous low salt solutions. To assess the RNA concentration and purity of each sample, the absorbance of each sample was measured at 260/280 and 260/230 nm by UV spectroscopy (Nanodrop 2000), respectively. The 260/280 ratio of RNA was around 2.0 and the 260/230 ratio was in the range of 2.0-2.2. The RNA concentration of the samples was at least 50 and at most 200 ng/µl.

3.6.3. Apoptosis assay by flow cytometry

Around 100.000 cells from control and TRAIL-treated macrophages from each donor were transferred to 1.5 mL of microcentrifuge tubes and centrifugated at 400 xg for 6 minutes at +4°C. Cells were washed twice with FACS buffer and centrifugated at 400 rcf for 5 minutes at +4°C. Master mix was prepared enough for the number of samples. 1.3 µl of Annexin V PE (BioLegend) and 1.3 µl 7AAD Viability Staining Solution PerCP-Cy5.5 (BioLegend) was mixed with 22.4 µl Annexin V binding buffer (BioLegend) for one sample and was multiplied with the number of samples. After the final wash is finished, the supernatant was discarded avoiding any extra fluid and for each sample, 25 µl of the master mix was added and mix well. All samples were incubated at RT for 15 minutes in the dark. After that, 100 µl of Annexin V binding buffer was added to each sample and acquisition was carried out by LSRFortessa (BD Biosciences) and the results were analyzed by FlowJo software version 10.4 (Tree Star). Cells were gated to exclude dead cells to measure the live macrophage population.

3.6.4. Characterization of TRAIL receptors in human primary monocytes by flow cytometry

Human primary monocytes of each donor after isolation were plated at a concentration of 6.5×10^5 cells per well in V-bottom 96-well plates. Cells were washed with 1X PBS and centrifugated twice at 500 rcf for 5 minutes at +4°C. Then, the cell pellet was resuspended with 1:1000 diluted Zombie UV dye (BioLegend) with 1X PBS and the cell was incubated on ice, in the dark, for 20 minutes. Fc receptors were blocked with 25 µl FACS buffer containing 1:200 diluted Human TruStain FcX antibody (Biolegend) for 15 minutes on ice after cells were washed and centrifuged with PBS. After that, cells were incubated for 45 minutes on ice in 25 µl of FACS buffer containing an antibody cocktail mix (anti-CD14-V500, anti-CD16-PE Dazzle 594, anti-DR4-APC, anti-DR5-PE, anti-DR4-PE-Cy7). Anti-DR4-APC, anti-DR5-PE, anti-DR5-APC, and anti-DR4-PE-Cy7 were diluted as 1 to 100; anti-CD14-V500 was diluted as 1 to 200; anti-CD16-PE Dazzle 594 was diluted as 1 to 800. Subsequently, 25 µl of FACS buffer with single dyes was added to the pertinent compensation samples. After twice 1X PBS washing, cells were suspended in 100 µl of BD Cytofix buffer on ice for 15 minutes to fix cells. 100 µl of FACS buffer was utilized to suspend the fixed cells after they had been centrifuged at 500 rcf for 5 minutes at +4°C. The experiment was carried out in the dark according to the manufacturer's protocol. The acquisition was performed by LSRFortessa (BD Biosciences) and the results were analyzed by FlowJo software version 10.4 (Tree Star).

3.6.5. RNA sequencing and differential gene expression analysis of both control and TRAIL-treated groups of macrophages

3.6.5.1. The preparation of the samples for RNA sequencing

The total RNA of each donor extracted in part of 3.6.2 named "*RNA Isolation* " were measured by Nanodrop 2000 to check their concentration and purity. Besides, the integrity of the RNA of each sample was determined by Agilent 2100 Bioanalyzer via RNA 6000 Nano Assay Reagent Kit before the sequencing procedure. It was observed that there was no degradation in the 28S and 18S ribosomal bands of the RNA samples to be sequenced. After checking RNA samples has appropriate molecular weight without any degradation of RNA, samples were sent for RNA-sequencing to Novogen located in Cambridge, England.

3.6.5.2. The workflow of RNA sequencing

12 RNA samples were prepared as 3 biological replicates of M0, TRAIL-treated M0, M1 and TRAIL-treated M1 groups. The first step in RNA sequencing involves converting the RNA into complementary DNA(cDNA) fragments to create a cDNA library. Once cDNA was obtained, overly abundant transcripts such as rRNAs and globin were removed by poly d(T) magnetic beads avoiding a decreased read depth of the sequencing. Following clearing our transcripts of interest, adaptors which are synthetic oligonucleotides were to be ligated onto the 3' or 5' end of cDNAs after that cDNAs with the new adaptors were PCR amplified to increase the concentration of the libraries. Before loading the samples to the sequencing, quality checks were done to ensure libraries are sequenced evenly and an overrepresented library is not present. Once quality control passed, libraries were loaded by ILLUMINA NextSeq 500 High Output v2 (150 cycles) kit to NextSeq 500 machine with 40 million (40 bp) reads and 150 PE read length and mode.

3.6.5.3. *RNA-seq data cleaning and editing*

Quality controls of reads of sequencing libraries were performed using FastQC software. Trimmomatic v0.39 software for removing adapter sequences from reads in Fastq file format. Sequences of the GRCh38 human reference genome were obtained in fasta format from the Ensembl database [https://www.ensembl.org/index.html/] and Rusbread v1.34.7 package command. Using this index created, ChIP sequencing reads "align(index={index file}, readfile1={input_1.fastq}, readfile2={input 2.fastq} type="RNA", input_format="gzFASTQ", output_format="BAM") ", output_file={output file}, nthreads=numParallelJobs)" is aligned to the corresponding reference genome. The obtained BAM files were then sorted with the sortBam() and indexBam() commands, respectively, and their indexes were created. Then, from the raw sequencing data "featureCounts(files = {infile.bam}, annot.ext = "{infile.gtf}", isGTFAnnotationFile = T, GTF.featureType = "exon", GTF.attrType = "gene_id", useMetaFeatures = T, countMultiMappingReads = T, isPairedEnd = T, nthreads = numParallelJobs)" command and parameters were used to determine gene level expression levels. Statistical significance of differences in gene expression level between groups was performed in the R computing environment (v3.5.2) with the edgeR package (v3.24.3). In this step, the count values determined by RSEM were normalized with The trimmed mean of M-values (TMM) normalization method and their statistical significance was calculated with the glmFit function by estimating the distribution with estimateDisp. Fragments Per Kilobase of transcript per Million (FPKM) values obtained from the featureCounts function and measured through the edgeR package were used to visualize the gene expression data. In the visualization of the expression data, the ggplot2 package was used in the R environment.

3.6.5.4. *Differential gene expression analysis*

This analysis was performed to determine the statistical significance of the differences in gene expression levels between the control and TRAIL-treated groups. To interpret the statistical significance of differences in gene expression level between groups, a script was written in the R computing environment (v3.5.2) using the edgeR package (v3.24.3). The purpose of this script is to determine the statistical significance of the raw count values determined by featureCounts by subjecting them to various processes. A data set suitable for analysis was obtained by using the raw count values of each sample. Then, all expression data from TRAIL-treated and control samples were compared with each other to find differentially expressed genes (DEGs). The top genes showing increasing and decreasing expression were acquired by setting a threshold of $FDR < 0.05$ and $|\log2FC(\text{Treated/Untreated})| > 0.6$. Then, heatmaps were drawn for easy interpretation of the expressions of each binary group.

Of the 12,749 genes interrogated in RNA-seq, 29 genes were significant in the comparison of TRAIL-treated M1 to M1 while 8 genes were significant in the comparison of TRAIL-treated M0 to M0 when sorted as mentioned above. Many of the genes are not known canonical genes of either differentiation or polarization in macrophages while a few of them are reported canonical genes of both M1 and M2 macrophages. LILRA5, CXCL11, HGF, and PACERR genes from the TRAIL M1 group and CXCL9, CXCL8, and CXCL5 from the TRAIL M0 group and TNF for both group were selected for further validation by qPCR.

3.6.6. qPCR confirmation of selected differentially expressed genes in TRAIL-treated groups of macrophages

3.6.6.1. RNA Isolation

For qPCR experiments, total RNA was isolated from eight biological replicates. All samples were prepared as indicated in part of 3.6.1 named "*Primary human monocyte-derived macrophage generation*". After the macrophage polarization step, lysis buffer containing β-mercaptoethanol (β-ME) (Sigma-Aldrich) was added to each well. Cell lysate of each sample was transferred to related microcentrifuge tubes and placed on ice. After harvesting all samples, cell lysate was loaded onto a QIAshredder spin column (QIAGEN) and placed in a 2 mL tube to homogenize the cells.

Homogenized cell lysate of each sample was transferred to a silica column and RNA binds to the silica while the rest of the other unnecessary constituents were washed out using a wash buffer including genomic DNA. In the last step, total RNA was eluted with 40 µl elution buffer from the silica beads via rehydrated with aqueous low salt solutions. To assess the RNA concentration and purity of each sample, the absorbance of each sample was measured at 260/280 and 260/230 nm by UV spectroscopy (Nanodrop 2000), respectively. The 260/280 ratio of RNA was around 2.0 and the 260/230 ratio was in the range of 2.0-2.2. The RNA concentration of the samples was at least 50 and at most 225 ng/µl.

3.6.6.2. cDNA synthesis

For RNA to cDNA synthesis, 1000 ng (1 ug) of total RNA from each sample was used and cDNA synthesis was carried out using EvoScript Universal cDNA Master. The main components of the synthesis include an RNA template, reverse transcriptase, reaction buffer containing dNTPs, DTT, RNase inhibitor, primer mix, and RNase-free water. Once all these components were mixed, the tube was loaded into a thermal cycler and incubated at 45°C for 15 minutes, at 85°C for 5 minutes, at 65°C for 15 min, and cooled to +4ºC with unlimited holding time. The cDNA samples were stored at -20°C and diluted 1:3 with RNase-free water for qPCR analysis.

3.6.6.3. qPCR validation of differential expressed genes

As mentioned in the 3.6.4.4 part, LILRA5, HGF, CXCL11, PACERR, CXCL9, CXCL8, CXCL5, and TNF were selected for further analysis by qPCR. Primers of reference gene and target genes were purchased as pre-designed PrimeTime qPCR assay(primer-probe mix) from IDT and the detailed information was listed in Table 4. A 3-fold dilution of the cDNA products of M0, TM0, M1, and TM1 of each donor was used as a template to perform qPCR analysis. Briefly, each well of the 96-well qPCR plate included 5 µl of 2X probe master mix of FastStart Essential DNA Probes Master, 1 µl of 10X PrimeTime qPCR assay, 1.5 µl of nuclease-free water and 2.5 of cDNA template for each target gene reaction. HPRT (hypoxanthine phosphoribosyltransferase 1) was used as a reference gene for all reactions. Three technical replicates were used for all measurements.

The qPCR was performed by using Applied Biosystems, StepOnePlus and 7500 Fast Real-Time PCR System and the following protocol was used: 10 mins of initial denaturation for activating the *Taq* polymerase at 95°C, 40 cycles of denaturation at 95°C for 10 sec, annealing and elongation at 60°C for 30 sec, and 1 cycle of cooling at 40°C for 30 sec. The $2^{-\Delta\Delta CT}$ method was used to assess the relative quantification (RQ) of gene expression and the results expressed as fold change.

Statistical analysis was performed by a one-tailed student t-test under the null hypothesis of whether there were no differences in the target gene expression between conditions.

3.6.7. Measurement of cytokine release

Cytokine production of macrophages was assessed using enzyme-linked immunosorbent assays (ELISA). The medium of each group of macrophages were collected and the levels of pro-inflammatory mediators TNF and CXCL11 were measured by sandwich ELISA according to the manufacturer’s instructions. Absorbance data were analyzed using a one-way Student’s t-test to determine significant differences between groups. Samples were run in duplicate.

3.7. Statistical Analysis

The data are shown as a mean ± SEM of at least 4 independent biological replicates and the statistical analysis of data was performed by using GraphPad Prism 9.0 (Graph-Pad Software). To compare the relative quantification of gene expression between conditions, the ROUT method and Shapiro-Wilk test were employed to identify outliers and to test the distribution of data. Paired Student’s t-test was performed under the null hypothesis that there were no differences in expression between conditions. These tests were performed for matched treatments, i.e. TRAIL-treated M0 vs M0, and TRAIL-treated M1 vs M1. Statistical significance was indicated by * meaning p-value < 0.05.

3.8. Research Plan

Macrophage apoptosis assay (November-December 2020)

↓

Characterization of TRAIL receptors in human primary monocytes (December 2020 - January 2021)

↓

Preparation of the samples to be sent for RNA-sequencing (February - May 2021)

↓

Quality control of the samples before RNA-sequencing procedure (June - August 2021)

↓

The analysis of RNA-sequencing data and determining differentially expressed genes (September - October 2021)

↓

Literature review for the top differentially expressed genes (October – November 2021)

↓

qPCR validation of the selected differentially expressed genes in Ireland and Turkey (December 2021 – August 2022)

↓

ELISA analysis of control (September 2022)

↓

Thesis writing (October – December 2022)

3.9. Limitation of Research

There was no obstacles in the study.

3.10. Ethics Committee Approval

The study was approved by the Non-Interventional Research Ethics Committee of Izmir Biomedicine and Genome Center on 25.06.2021 with protocol number 2021-017. The approval document has been attached in Section 8.1.

4. RESULTS

4.1. The expression of TRAIL receptors, DR4 and DR5, on human primary monocytes

Before investigating the role of TRAIL on human monocyte to macrophage differentiation, we first analyzed the cell surface expression of death receptors, DR4/TRAIL-R1 and DR5/TRAIL-R2, on primary human monocytes by using flow cytometry. Human primary monocytes are sub-divided into four populations based on CD16 and CD14 expression as $CD14^{+}CD16^{-}$, $CD14^{+}CD16^{intermedite}$, $CD14^{-}CD16^{+}$ and $CD14^{-}CD16^{++}$(Boyette et al., 2017; Passlick et al., 1989).The primary human monocytes were isolated from buffy coats of healthy donors and the DR4 and DR5 expression was analyzed on four monocyte subsets.

The DR4 was expressed on all monocyte subsets with the highest level of expression on $CD14^{-}CD16^{++}$ monocytes. The DR5 expression was barely detectable on $CD14^{-}CD16^{+}$ monocytes and the expression level was the highest on $CD14^{+}CD16^{-}$ compared to the other subsets.

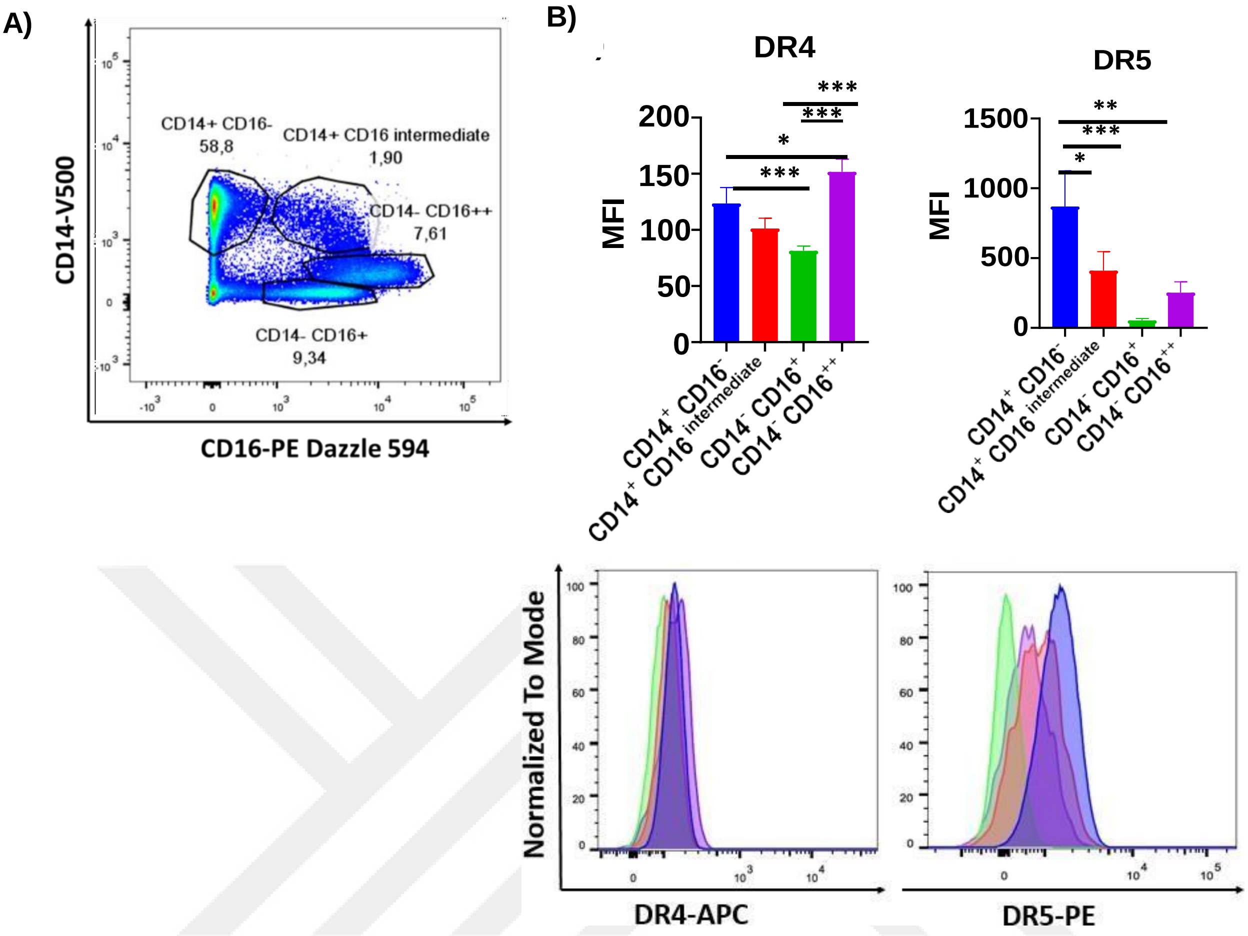

Figure 4. Evaluation of the cell surface expression of TRAIL receptors, DR4 and DR5 on monocyte subsets.

DR4/DR5 expression on isolated human primary monocytes was analyzed by flow cytometry. A) Monocyte subsets were gated based on their CD16 and CD14 expression. B) DR4/DR5 expression for each monocyte subset represented via bar graphs and histograms; results are shown mean ± SEM of biological replicates of 6 donors. Numbers in plots indicate mean fluorescence intensity. Statistical analysis: *P<0.05, **P<0.01, ***P<0.001 (one-way ANOVA).

4.2. Cell viability analysis

Next, we tested whether TRAIL induces apoptosis during monocyte to macrophage differentiation since TRAIL is known for its role in inducing cell apoptosis. Primary human monocytes were treated, along with M-CSF, with TRAIL or left untreated (control group) during macrophage differentiation for 7 days. Macrophages of both control and TRAIL-treated groups from each donor were stained with Annexin V and 7AAD at the end of 7-day differentiation and analyzed by flow cytometry. As depicted in Figure 2, the cell viability percentage (Annexin V-7AAD) of untreated M0 (unpolorized) macrophages, cultured only M-CSF was 93.07% while TRAIL-treated M0 macrophages, cultured with M-CSF and TRAIL, were 90.07%. The cell viability of the two groups was nearly the same and the statistical analysis under the null hypothesis that the difference between the two groups is the same was non-significant meaning the null hypothesis is accepted.

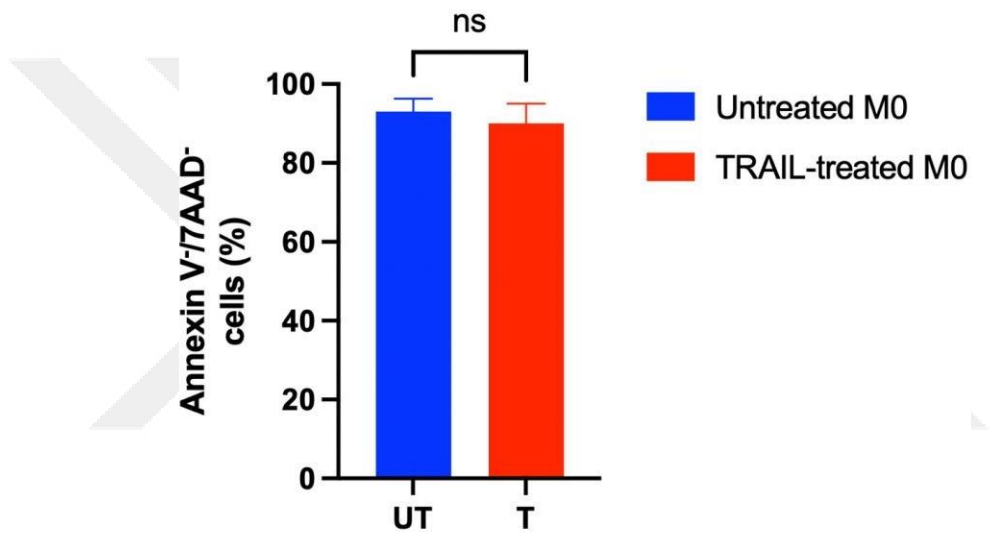

Figure 5. The cytotoxic activity of rhTRAIL on macrophages.

The cytotoxic effect of rhTRAIL on macrophages was quantitatively evaluated by flow cytometry after AnnexinV&7AAD staining. Primary human monocytes were left untreated or were treated for 7 days with 10 ng/mL M-CSF and 200 ng/mL rhTRAIL ; results are shown as % of alive cells (Mean ± SE of 4 donors). Statistical analysis: ns: non-significant (Student's t-test).

4.3. Quality control of RNA samples of experimental groups

In order to characterize the gene expression profile of differentiation of primary human monocytes to mature macrophages in the presence of TRAIL and subsequent polarization to M1, primary human monocytes from 3 healthy donors were isolated. Freshly isolated monocytes from each donor were divided into two groups that one group was only cultured with 10 ng/mL M-CSF and the other group was cultured with 200 ng/mL TRAIL and 10 ng/mL M-CSF for 7 days. After 7 days, both treated and untreated mature macrophages were also divided into two groups that one group was left as unpolarized, M0 macrophages while the other group was polarized to M1 macrophages with LPS and IFN-γ for 5 hours. For only one donor, there were 4 groups as following; M0, TRAIL-treated M0, M1 and TRAIL-treated M1 so that totally 12 groups were prepared for RNA-sequencing. The total RNA of these 12 samples were extracted with a commercial kit. The total RNA quality of samples was assessed by measuring the 28S/18S ribosomal RNA(rRNA) and the RNA Integrity Number(RIN) with Agilent Bioanalyzer 2100 using RNA 6000 Nano Chips (**Figure 6**).

A)

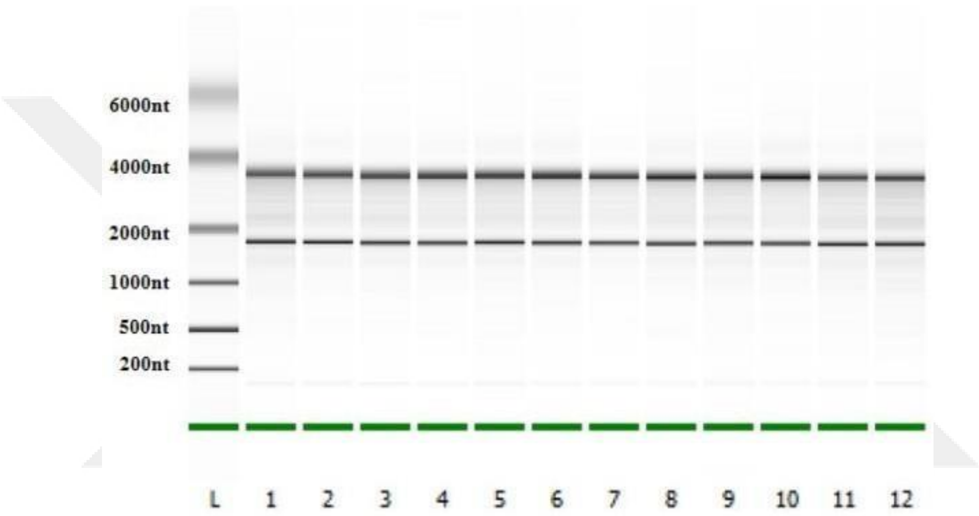

B

D1-M0

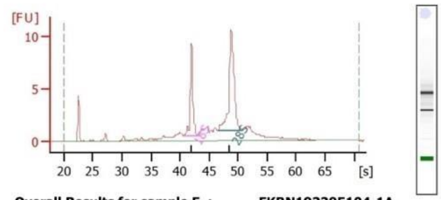

Overall Results for sample 5 : **FKRN192295104-1A**

RNA Area:	70.1
RNA Concentration:	129 ng/µl
rRNA Ratio [28s / 18s]:	1.9
RNA Integrity Number (RIN):	8.9 (B.02.08)
Result Flagging Color:	
Result Flagging Label:	RIN: 8.90

Fragment table for sample 5 : **FKRN192295104-1A**

Name	Start Time [s]	End Time [s]	Area	% of total Area
18S	40.63	43.00	10.4	14.8
28S	46.59	50.70	19.8	28.3

D1-TM0

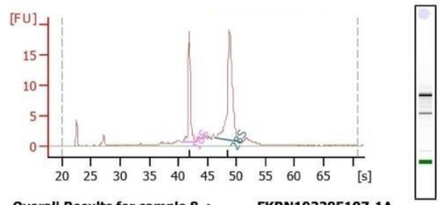

Overall Results for sample 8 : **FKRN192295107-1A**

RNA Area:	97.8
RNA Concentration:	181 ng/µl
rRNA Ratio [28s / 18s]:	2.1
RNA Integrity Number (RIN):	9.5 (B.02.08)
Result Flagging Color:	
Result Flagging Label:	RIN: 9.50

Fragment table for sample 8 : **FKRN192295107-1A**

Name	Start Time [s]	End Time [s]	Area	% of total Area
18S	40.63	43.05	18.5	18.9
28S	46.39	50.80	38.0	38.8

D1-M1

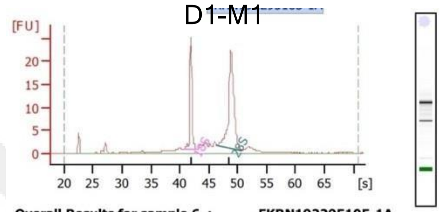

Overall Results for sample 6 : **FKRN192295105-1A**

RNA Area:	124.2
RNA Concentration:	229 ng/µl
rRNA Ratio [28s / 18s]:	1.9
RNA Integrity Number (RIN):	9.4 (B.02.08)
Result Flagging Color:	
Result Flagging Label:	RIN: 9.40

Fragment table for sample 6 : **FKRN192295105-1A**

Name	Start Time [s]	End Time [s]	Area	% of total Area
18S	40.68	43.10	24.2	19.5
28S	46.39	50.70	46.8	37.7

D1-TM1

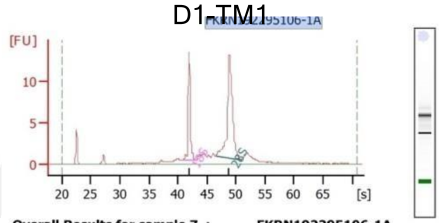

Overall Results for sample 7 : **FKRN192295106-1A**

RNA Area:	76.3
RNA Concentration:	141 ng/µl
rRNA Ratio [28s / 18s]:	2.0
RNA Integrity Number (RIN):	9.4 (B.02.08)
Result Flagging Color:	
Result Flagging Label:	RIN: 9.40

Fragment table for sample 7 : **FKRN192295106-1A**

Name	Start Time [s]	End Time [s]	Area	% of total Area
18S	40.63	43.10	13.2	17.3
28S	46.49	50.80	26.7	34.9

C

D2-M0

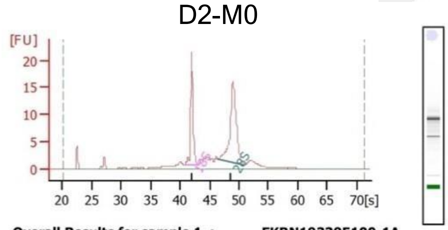

Overall Results for sample 1 : **FKRN192295100-1A**

RNA Area:	118.3
RNA Concentration:	218 ng/µl
rRNA Ratio [28s / 18s]:	1.7
RNA Integrity Number (RIN):	9.2 (B.02.08)
Result Flagging Color:	
Result Flagging Label:	RIN: 9.20

Fragment table for sample 1 : **FKRN192295100-1A**

Name	Start Time [s]	End Time [s]	Area	% of total Area
18S	40.71	43.09	22.1	18.7
28S	46.45	50.84	37.6	31.8

D2-TM0

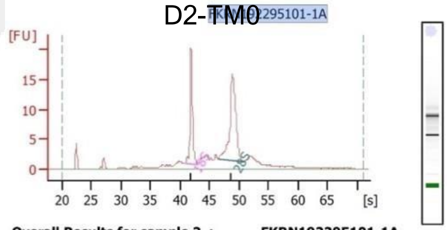

Overall Results for sample 2 : **FKRN192295101-1A**

RNA Area:	118.0
RNA Concentration:	218 ng/µl
rRNA Ratio [28s / 18s]:	1.7
RNA Integrity Number (RIN):	9.2 (B.02.08)
Result Flagging Color:	
Result Flagging Label:	RIN: 9.20

Fragment table for sample 2 : **FKRN192295101-1A**

Name	Start Time [s]	End Time [s]	Area	% of total Area
18S	40.73	42.94	20.9	17.7
28S	46.44	50.82	35.9	30.4

D2-M1

FKRN192295103-1A

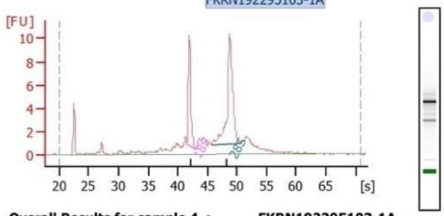

Overall Results for sample 4 : **FKRN192295103-1A**

RNA Area:	73.6
RNA Concentration:	136 ng/µl
rRNA Ratio [28s / 18s]:	2.1
RNA Integrity Number (RIN):	8.6 (B.02.08)
Result Flagging Color:	
Result Flagging Label:	RIN: 8.60

Fragment table for sample 4 : **FKRN192295103-1A**

Name	Start Time [s]	End Time [s]	Area	% of total Area
18S	41.51	42.89	9.8	13.3
28S	45.72	50.70	20.7	28.2

D2-TM1

FKRN192295102-1A

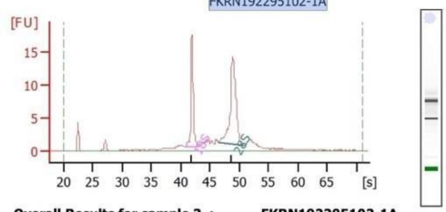

Overall Results for sample 3 : **FKRN192295102-1A**

RNA Area:	95.0
RNA Concentration:	175 ng/µl
rRNA Ratio [28s / 18s]:	1.8
RNA Integrity Number (RIN):	9.4 (B.02.08)
Result Flagging Color:	
Result Flagging Label:	RIN: 9.40

Fragment table for sample 3 : **FKRN192295102-1A**

Name	Start Time [s]	End Time [s]	Area	% of total Area
18S	40.73	42.99	17.7	18.6
28S	46.44	50.82	31.7	33.4

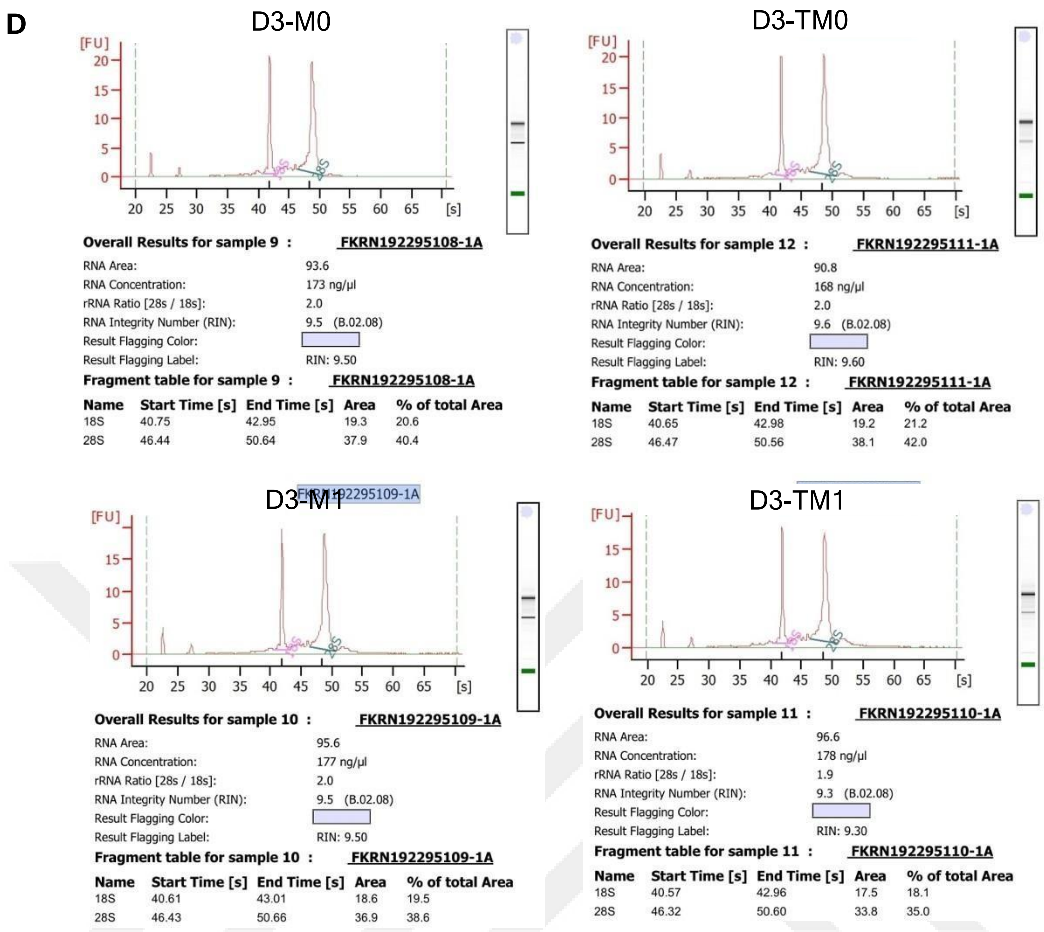

Figure 6. Evaluation of the RNA integrity of experimental groups.

The quality of RNA samples was measured by 28S to 18S rRNA ratio through agarose gel electrophoresis and further processed by Agilent Bioanalyzer 2100. **A)** Gel image showing two bands comprising the 28S and 18S rRNA of the related sample. **B, C, D)** RIN values of each donor UT-M0, TM0, M1, and TM1, respectively.

4.4. Characterization of M0 and M1 macrophages by RNA-seq-based gene expression profiling

The gene expression profiling of TRAIL-treated and untreated M0 and M1-polarized macrophages from three healthy donors was performed by RNA sequencing. To assess inter- and intragroup variability, PCA (principal component analysis) (**Figure 7.A**) and hierarchical clustering (**Figure 7.B**) based on differentially expressed genes were performed and showed segregation of the samples by treatment and polarization state. The grouping among replicates within samples and sample groups spread across two axes was demonstrated in the PCA plot. PCA plot reveals 55.94% of the total variance of the complete data set lies within the first two components. Macrophage polarization was associated with significant changes in transcriptional level around ~ 42% of the total variance, followed by slightly smaller changes associated with TRAIL treatment, although one donor was very different than other donors. Moreover, Spearman's correlation matrix visualized as a heat map reflects the correlation between two samples. Both the color and the size of the square indicate the correlation coefficient so that a larger square with dark blue color indicates similar expression profiles between the two samples. The diagonal of the correlation plot has only dark blue color that illustrates matching the sample with itself. The correlation value lies between 0.7 and 0.9 which means that any two samples have a strongly positive relationship. The most diverse samples are the unpolarized sample (M0) and polarized sample (M1) since the square has the smallest size and light blue color whereas the most similar samples are the different donors in the same group.

A)

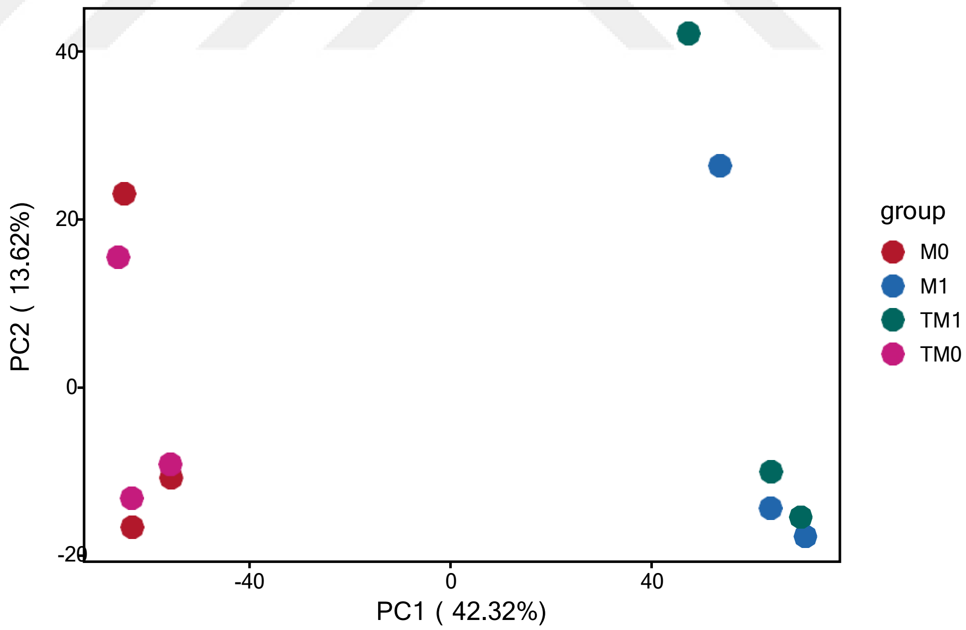

B

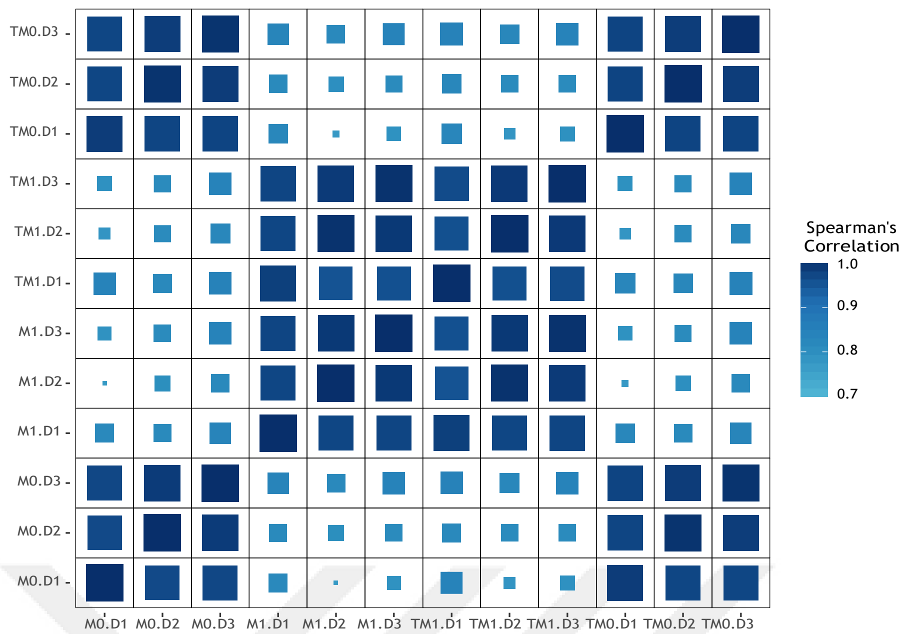

Figure 7. Transcriptional profiling of experimental groups.

A) PCA plot displaying four groups which are M0, TRAIL-treated M0, M1 and TRAIL-treated M1 of three donors along PC1 and PC2, reflecting expression trends within the data set. Each color represents each experimental group. **B)** Spearman's correlation heat map visualizes the correlation between samples. The color and the size of the square indicate how strong correlation between each pair in the data set. The range of correlation coefficients is displayed as a scale bar on the right side.

4.5. Differentially expressed gene analysis

To characterize a high-resolution map of transcriptome response to TRAIL treatment in macrophages, we identified 29 and 8 differentially expressed genes relative to the control in M0 and M1 groups, respectively (|log2FC| > 0.6 at FDR < 0.05, see **Table 8 and Table 9**), including known pro-inflammatory markers in activated macrophages.

The MA (ratio intensity) plot with log fold-change (logFC) along against log counts per million(logCPM) allows for the analysis of data normalization and the visualization of sample reproducibility (McDermaid et al., 2018). As seen in **Figure 8.A** and **8.B**, data points falling above 1 along the y axis, indicate the genes being upregulated while below -1 indicates the genes being downregulated and genes not being significantly expressed are presented around the horizontal line. Red dots represent upregulated significant genes; blue dots represent downregulated significant genes; grey dots represent non-significant genes. 3 upregulated genes and 4 downregulated genes were present in **Figure 8.A** 18 of upregulated genes and 10 downregulated genes are present in **Figure 8.B.** Totally, there were barely significantly differentially expressed genes present since most of the genes lie around the horizontal line which means that the transcriptome profile of two samples (control and treated sample either M0 or M1) is similar.

Heatmap visualization provides a global overview of the gene expression pattern of all samples, allowing for the determination of genes to be further investigated. In **Figure 9.A** and **9.C**, the expression data is shown as a grid with each row representing a differentially expressed gene and each column representing a sample. As depicted in the legend on the right side, relative changes in gene expression are shown by the color and its intensity of the boxes. Up-regulated genes are represented by red color whereas down-regulated genes are shown by blue color. The yellow color represents a gene whose expression has not changed. The tree resulting from hierarchical clustering plotted left side of the heat map shows the similarity between gene expressions means that higher similarity between different genes' expression shorter connecting lines.

A)

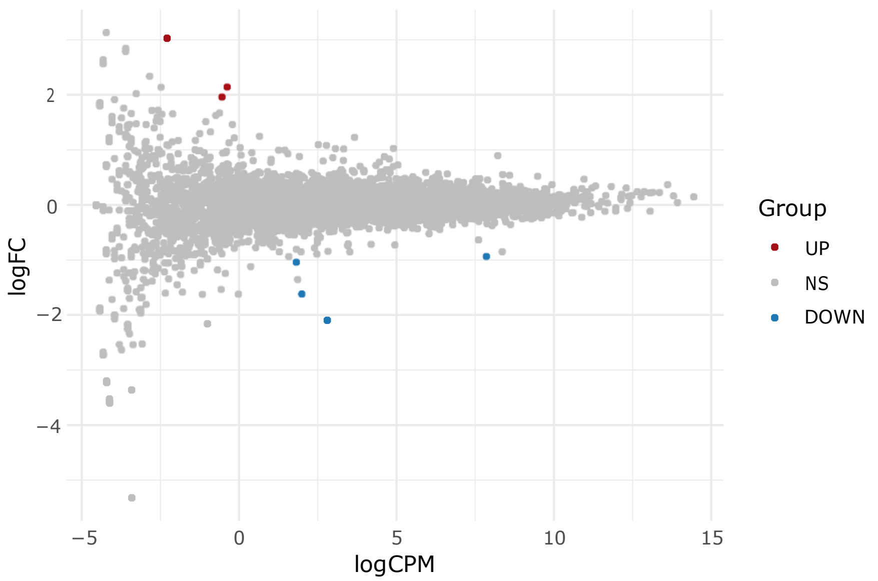

B

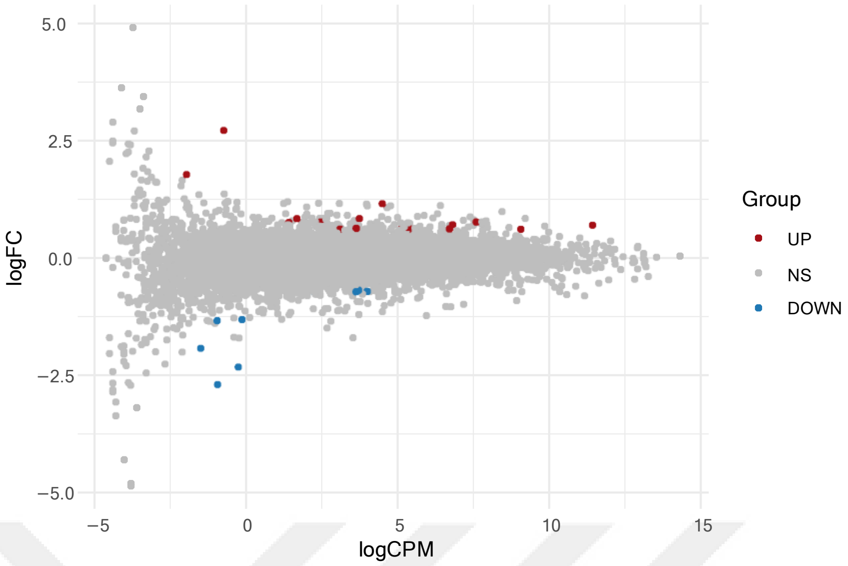

Figure 8. MA plot illustrates the distribution of the identified differentially expressed genes between control groups and TRAIL-treated groups.
UP(red) and DOWN(blue) represent upregulated and downregulated transcripts, respectively. NS(grey) represent non-significant genes. **A)** MA plot of TRAIL-treated M0 versus M0. **B)** MA plot of TRAIL-treated M1 versus M1.

A)

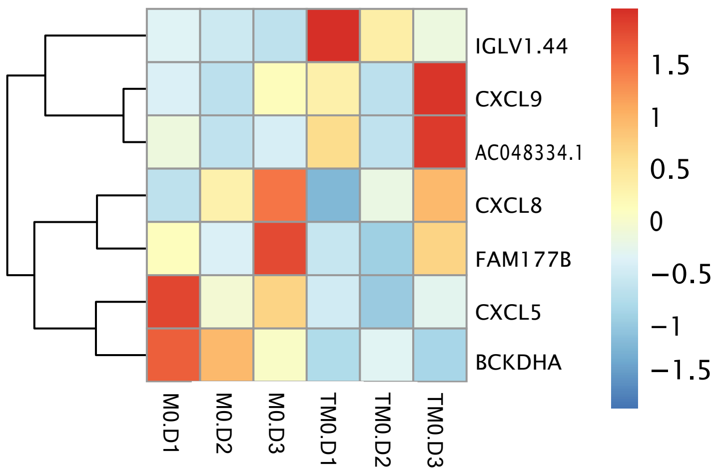

B)

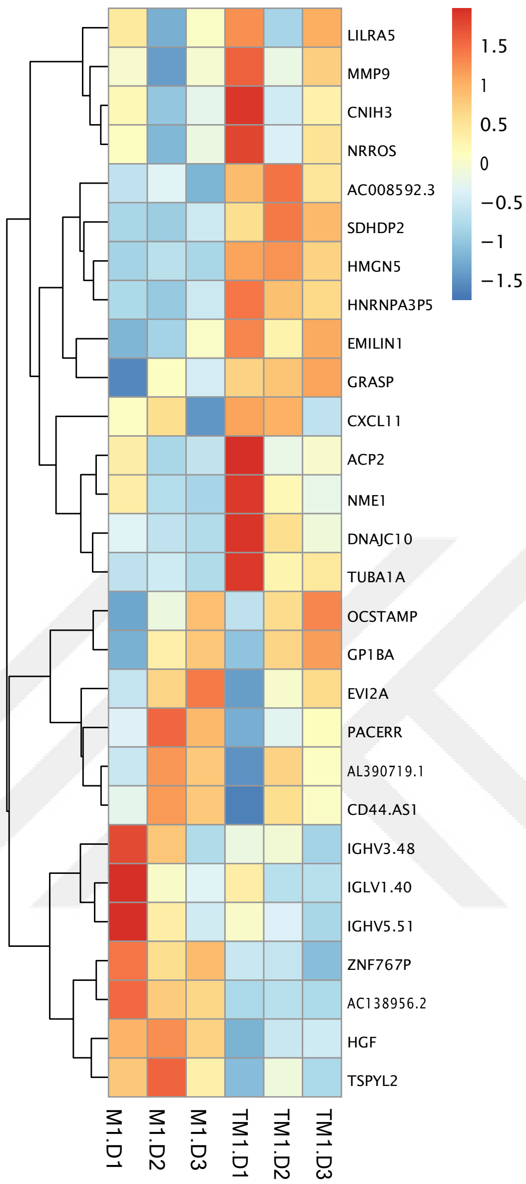

Figure 9. Visualization of transcriptome profiles of samples in a heatmap showing the top enriched genes.

A) Chart of TRAIL-treated M0 versus M0. **B)** Chart of TRAIL-treated M1 versus M1. Squares are color-coded; red(upregulated) and blue(downregulated).

The volcano plot (**Figure 10**) is another way to visualize every single gene in the comparison through the statistical significance of the difference (p-value) relative to the magnitude of difference (fold change), usually in the negative base-10 p-value and base-2 log fold change, respectively. The upregulated genes are towards the right of the plot while the downregulated genes are towards the left of the plot and as the gene shifts to the top of the plot, its significance increases. **In Figure 10.A**, 7 differentially expressed genes are plotted in the comparison of TRAIL-treated M0 versus untreated M0, whilst 29 differentially expressed genes are plotted in the comparison of TRAIL-treated M1 versus untreated M1 in **Figure 10.B**. Although some genes meet the p-value threshold which is displayed by blue points, data points closer to 0 along the x-axis represent genes that have a similar expression in both the control group and treatment group.

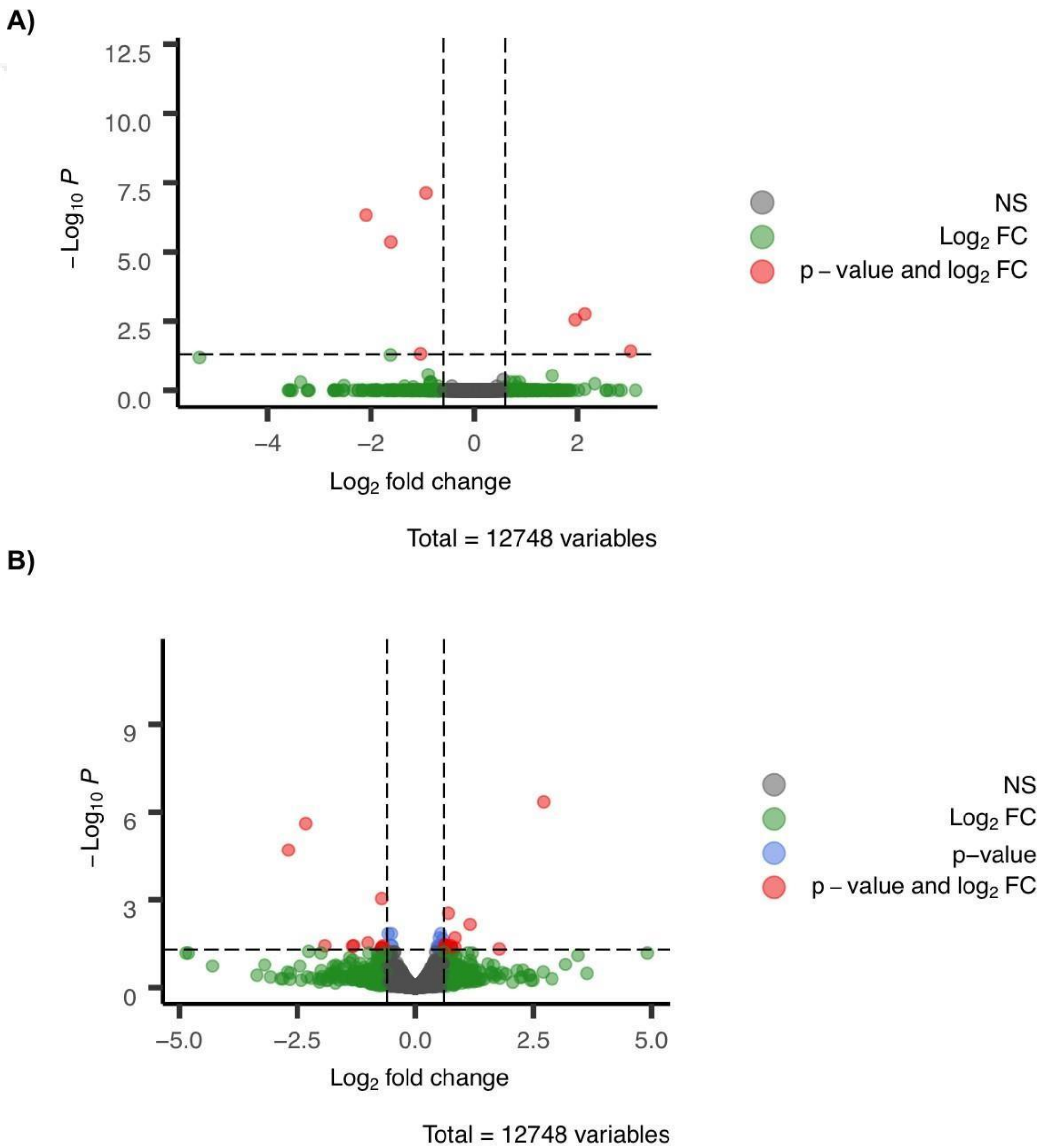

Figure 10. Volcano plot of RNA-seq dataset of experimental groups.
One gene is represented by a point. Each point corresponds to one gene. DEGs with |log2FC| > 0.6 and $p < 0.05$ are shown in red, whilst non-significant genes are highlighted by grey points. **A)** Plot of TRAIL-treated M0 versus M0. **B)** Plot of TRAIL-treated M1 versus M1.

To investigate whether TRAIL had a functional consequence on macrophage differentiation, After applying $\log_2$FC and FDR cutoff, genes were ranked based on differential expression. 7 genes of the M0 group and 29 genes of the M1 group were depicted in **Table 8** and **Table 9**, respectively. For further analysis by qPCR, CXCL9, CXCL8, CXCL5, and TNF from the M0 dataset and LILRA5, CXCL11, HGF, PACERR and TNF from the M1 dataset are selected.

In **Table 8**, CXCL9, CXCL8, and CXCL5 genes belong to the CXC chemokine family in the M0 group. CXCL9 is upregulated while CXCL8 and CXCL5 are downregulated. Although most of the genes are protein coding, the AC048334.1 gene which is highly differential in M0 dataset is an unprocessed pseudogene (GTEx Consortium, 2013).

In **Table 9,** LILRA5 and CXCL11 were upregulated and HGF and PACERR were downregulated in TRAIL-treated M1 compared to the control. LILRA5 is a member of the leukocyte immunoglobulin-like receptor subfamily and the LIR family members are generally involved in regulatory functions in leukocytes as LILRA5 is highly homologous to other LILR genes (Brown, Trowsdale, & Allen, 2004; Borges, Kubin, & Kuhlman, 2003). CXCL11 is a well-known pro-inflammatory chemokine belonging to the CXC chemokine family (Cole et al., 1998). HGF, hepatocyte growth factor, contributes to cell growth, cell motility, and morphogenesis in various cell types (Sakai et al., 2014). PACERR is a long non-coding RNA that promotes the expression of cyclooxygenase2 (COX2) product, prostaglandin-endoperoxide synthase 2 (PTGS2) (Tian et al., 2016). ACP2 and EMILIN1 genes are selected as backup. ACP2 is an acid phosphatase located generally in the lysosomes of phagocytes (Xu et al., 2012). EMILIN1 is an extracellular matrix protein, preventing TGF-ß maturation by binding pro-TGF-ß precursor (Zacchigna et al., 2006).

Table 8. The top differentially expressed genes in the M0 group.

Gene Name	Gene Symbol	Log_2FC	FDR	Up/Down
Pseudogene	AC048334.1	3.031	0.039	+8.171
Immunoglobulin lambda variable 1-44	IGLV1-44	2.139	0.002	+4.405
C-X-C motif chemokine ligand 9	CXCL9	1.958	0.003	+3.884
C-X-C motif chemokine ligand 8	CXCL8	-0.933	0.000	-1.910
Branched-chain keto acid dehydrogenase E1 subunit alpha	BCKDHA (MSU, OVD1A)	-1.038	0.048	-2.054
Family with sequence similarity 177 member B	FAM177B	-1.615	0.000	-3.063
C-X-C motif chemokine ligand 5	CXCL5	-2.095	0.000	-4.271

Table 9. The top differentially expressed genes in the M1 group.

Gene Name	Gene Symbol	Log_2FC	FDR	Up/Down
Succinate Dehydrogenase Complex Subunit D Pseudogene 2	SDHDP2	2.716	0.000	+6.572
Pseudogene	AC008592.3	1.777	0.048	+3.427
General receptor for phosphoinositides 1 associated scaffold protein	GRASP (TAMALIN)	1.157	0.007	+2.230

Cornichon family AMPA receptor auxiliary protein 3	CNIH3	0.840	0.043	+1.790
Nucleoside diphosphate kinase A	NME1(NM23-H1)	0.840	0.020	+1.790
Tubulin alpha 1a	TUBA1A	0.768	0.043	+1.703
Osteoclast stimulatory transmembrane protein	OCSTAMP	0.766	0.046	+1.700
High mobility group nucleosome binding domain 5	HMGN5 (NSBP1,NBP-45, GARP45)	0.756	0.037	+1.689
Acid phosphatase 2	ACP2 (LAP)	0.709	0.043	+1.635
Matrix metalloproteinase 9	MMP9	0.700	0.003	+1.625
Negative regulator of reactive oxygen species	NRROS (Lrrc33)	0.656	0.037	+1.575
DnaJ heat shock protein family (Hsp40) member C10	DNAJC10	0.641	0.040	+1.559
Glycoprotein Ib platelet alpha subunit	GPIbα (CD42b)	0.632	0.043	+1.550
Leukocyte immunoglobulin-like receptor A5	LILRA5 (LIR9,CD85)	0.622	0.034	+1.539
C-X-C motif chemokine ligand 11	CXCL11	0.614	0.035	+1.530
Heterogeneous nuclear ribonucleoprotein A3 pseudogene 5	HNRNPA3P5	0.613	0.043	+1.530
Elastin microfibril interfacer 1	EMILIN1	0.608	0.043	+1.524
Pseudogene	AL390719.1	-0.684	0.037	-1.606

Zinc finger family member 767	ZNF767P	-0.696	0.043	-1.620
Ecotropic viral integration site 2A	EVI2A	-0.710	0.001	-1.636
Testis-specific Y-encoded-like protein 2	TSPYL2	-0.715	0.043	-1.642
CD44 antisense RNA 1	CD44-AS1	-0.717	0.046	-1.644
Hepatocyte growth factor	HGF	-1.006	0.030	-2.008
PTGS2 antisense lncRNA	PACERR (PACER, PTGS2-AS1)	-1.309	0.037	-2.479
Pseudogene	AC138956.2	-1.331	0.038	-2.515
Immunoglobulin heavy variable 3-48	IGHV3-48	-1.920	0.037	-3.785
Immunoglobulin lambda variable 1-40	IGLV1-40	-2.320	0.000	-4.992
Immunoglobulin heavy variable 5-51	IGHV5-51	-2.692	0.000	-6.460

4.5. qPCR validation of selected DEGs

4.5.1. qPCR validation of selected DEGs in M0 groups

To confirm the credibility of DEGs obtained from RNA-seq, CXCL9, CXCL8, CXCL5, and TNF gene expression was analyzed by qPCR using a total RNA sample of at least 4 different donors. Although the TNF gene was upregulated (logFC is 0.083) but the FDR value was higher than 0.05, but its expression was also checked by qPCR. The expression patterns of CXCL9, CXCL8, and TNF were concordant with RNA-seq results (**Figure 11.A, 11.B** and **11.C**). Although, the CXCL5 expression was decreased similar to the RNA-seq result, it did not reach statistical significance in the TRAIL-treated M0 macrophage (**Figure 11.D**).

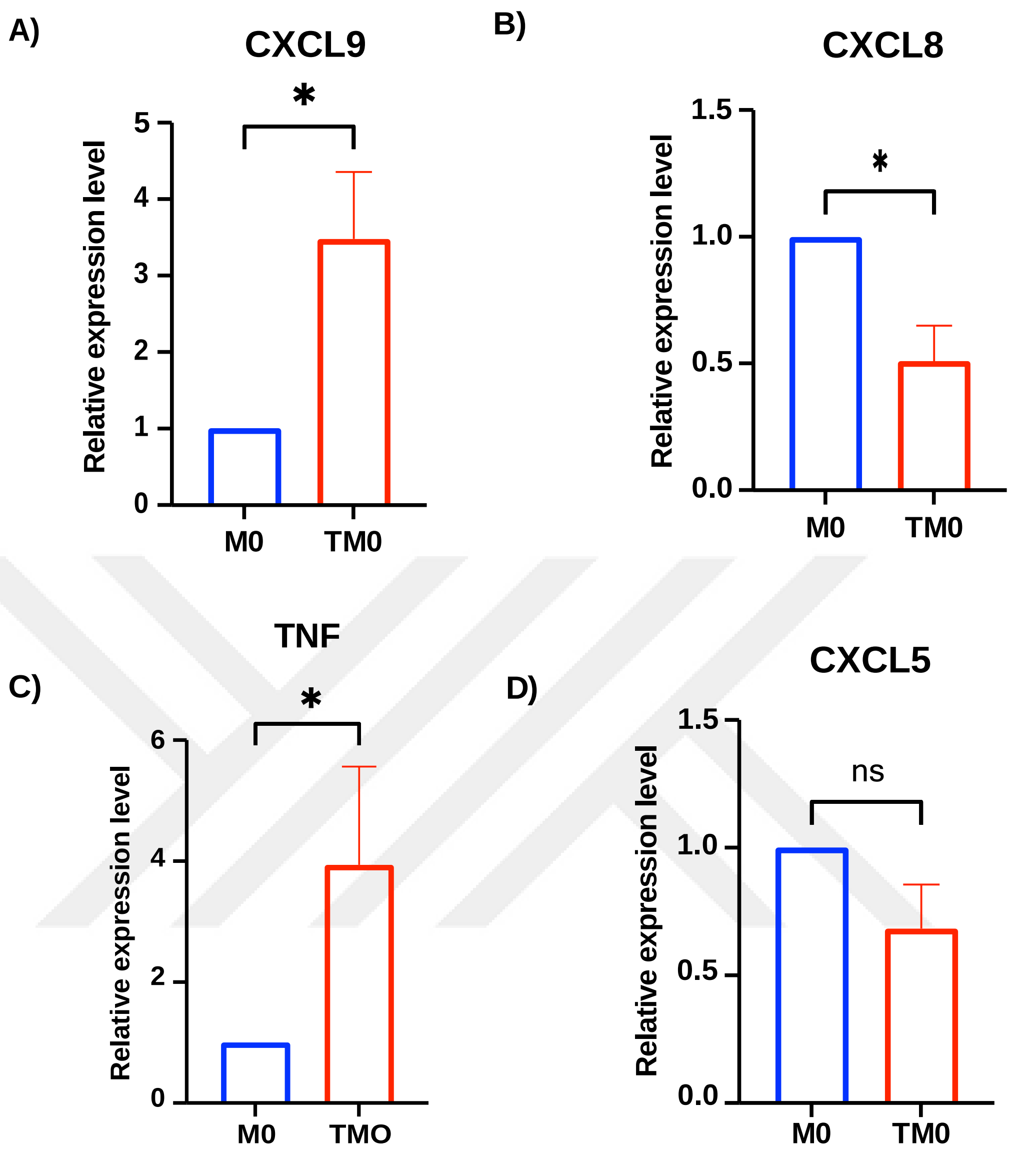

Figure 11. qPCR results of selected DEGs from RNA-seq dataset of M0 group. The relative expression level(fold change) in both M0 (blue) and TRAIL-treated M0 (red) groups are shown. **A)** CXCL9 **B)** CXCL8 **C)** TNF **D)** CXCL5. The relative expression levels were calculated based on the expression level of the reference gene, HPRT, using the formula $2^{-\Delta\Delta Ct}$. Data is shown by mean ± SEM of at least 4 different independent biological replicates. A statistically significant difference ($p < 0.05$), as assessed by the student's paired t-test and Wilcoxon test, is depicted by an asterisk (*); ns: not significant.

4.5.2. qPCR validation of selected DEGs in M1 groups

The expression of CXCL11, LILRA5, HGF, PACERR and TNF were investigated by qPCR using a total RNA sample of at least 4 different donors to confirm the credibility of DEGs obtained from RNA-seq. Although, the TNF gene was downregulated (logFC is -0.534) but the FDR value was higher than 0.05, its expression was also checked by qPCR. Surprisingly, although the RNA-seq analysis showed increased expression of CXCL11 and LILRA5 in the TRAIL-treated M1 macrophages, CXCL11 expression was decreased and LILRA5 expression was comparable to control when analyzed by qPCR (**Figure 12.A and 12.B**). The expression patterns of HGF and PACERR were concordant with RNA-seq results (**Figure 12.C** and **12.D**). Although, the TNF expression was downregulated in RNA-seq data of the TRAIL-treated M1 group, the expression of TNF was upregulated when analyzed by qPCR (**Figure 12.E**).

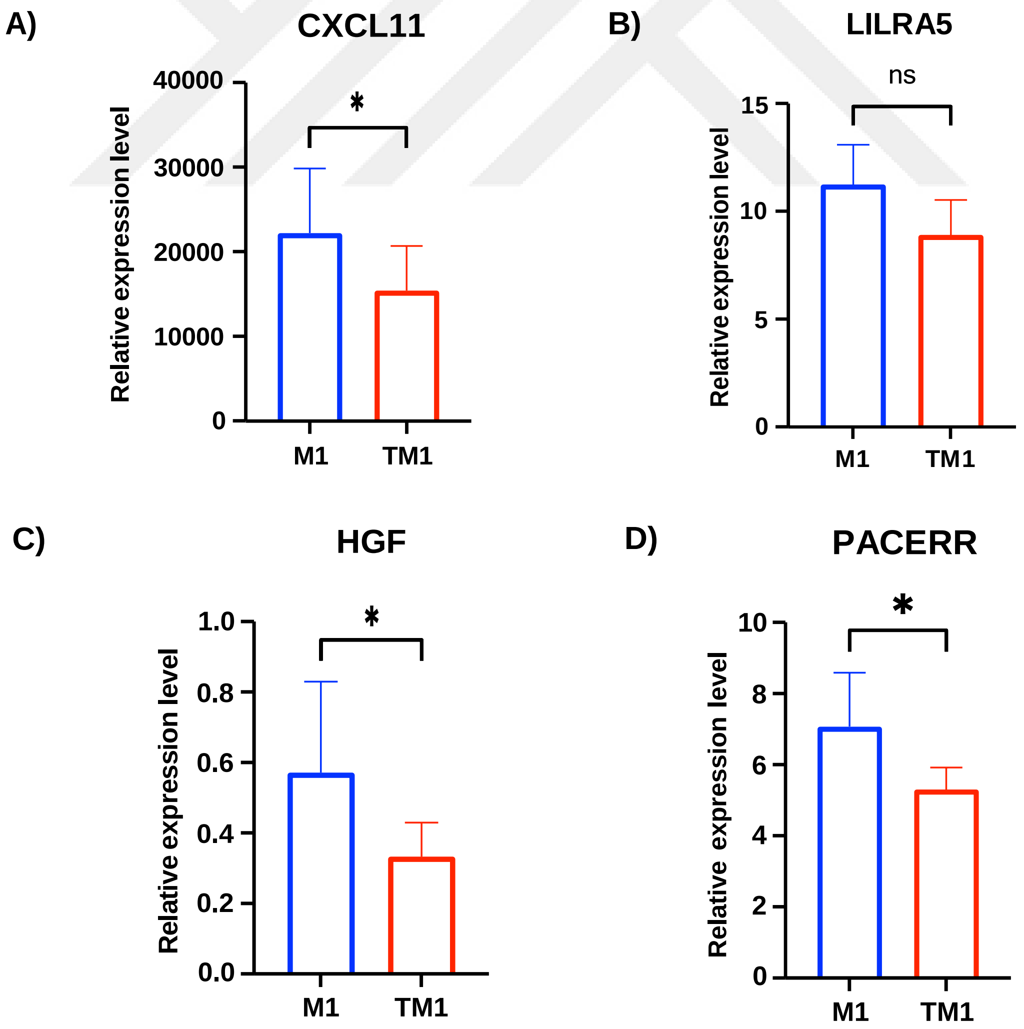

E)

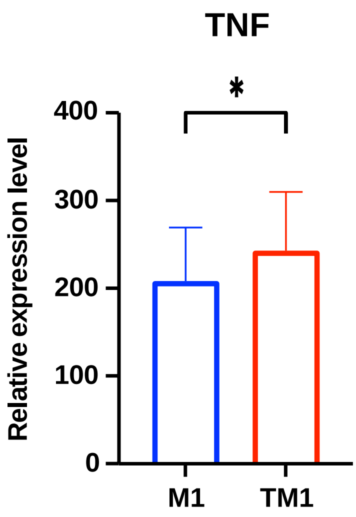

Figure 12. qPCR results of selected DEGs from the RNA-seq dataset of the M1 group.

The relative expression level (fold change) in both M1 (blue) and TRAIL-treated M1 (red) groups are shown. **A)** CXCL11 **B)** LILRA5 **C)** HGF **D)** PACERR **E)** TNF. The relative expression levels were calculated based on the expression level of the reference gene, HPRT, using the formula $2^{-\Delta\Delta Ct}$. Data is shown by mean ± SEM of at least 4 different independent biological replicates. A statistically significant difference ($p < 0.05$), as assessed by the student's paired t-test is depicted by an asterisk (*); ns: not significant.

4.6. Analysis of TNF and CXCL11 by ELISA

Next, we investigated the impact of TRAIL on monocyte to macrophage differentiation at protein level. TNF and CXCL11 levels of TRAIL treated and control M0 and M1 macrophages was analyzed by ELISA.

The level of TNF was increased in the TRAIL-treated M1 group compared to the control similar to the results of gene expression (**Figure 13.A**). In M0 macrophages, although the TNF gene expression was detected , the cytokine level of TNF could not be detected due to the cytokine level being below the detection range. Cytokine level of CXCL11 was elevated in both TRAIL-treated M0 and M1 groups.

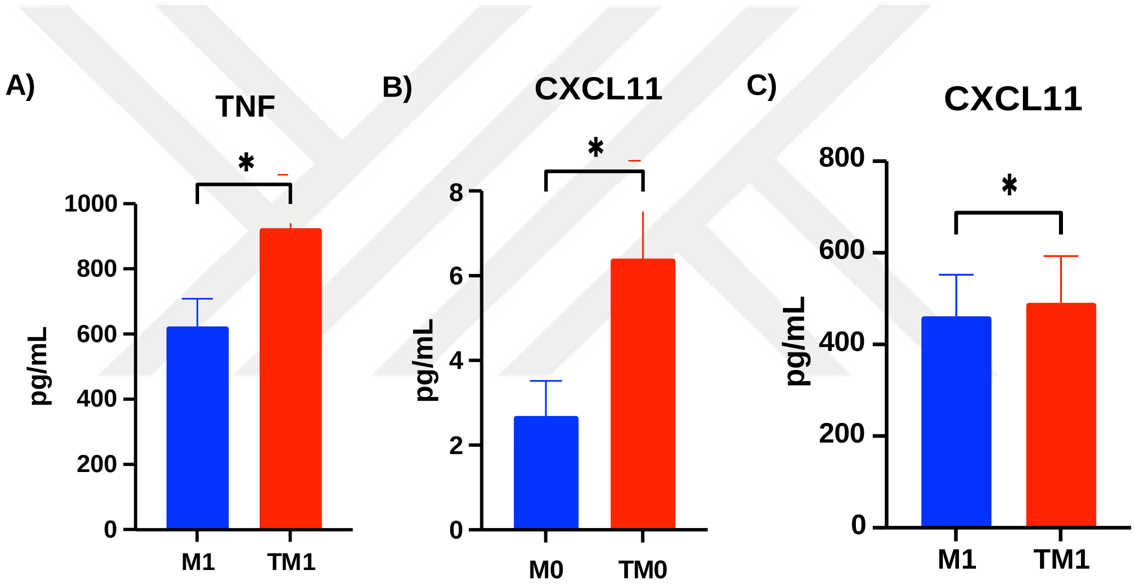

Figure 13. Impact of TRAIL on TNF and CXCL11 production by macrophages. The cytokine level (pg/mL) in both M0 and M1 groups is shown. **A)** TNF in M1 group **B)** CXCL11 in M0 group **C)** CXCL11 in M1 group. Data is shown by mean ± SEM of 4 different independent biological replicates. A statistically significant difference ($p < 0.05$), as assessed by the student's t-test is depicted by an asterisk (*)

5. DISCUSSION

In this study, we performed a comprehensive analysis of TRAIL receptor expression on monocyte subsets together with susceptibility of macrophages to TRAIL-mediated apoptosis and the immunoregulatory function of TRAIL signaling in monocyte to macrophage differentiation.

5.1. TRAIL receptor expression on primary human monocytes

Before rhTRAIL treatment, we investigated whether the monocyte populations express functional TRAIL receptors, DR4 and DR5, on their surfaces. In monocyte subsets, classical monocytes comprise about 59% of the total monocyte population and the rest of the population, approximately 41%, is composed of non-classical and intermediate monocyte subsets (**Figure 4**). DR4 (TRAIL-R1) expression is the highest in non-classical ($CD14^{-}CD16^{++}$) and gradually decreased following $CD14^{+}CD16^{-}$, $CD14^{+}CD16^{intermediate}$, $CD14^{-}CD16^{+}$ monocyte subsets while DR5 expression is the highest in classical monocytes ($CD14^{+}CD16^{-}$) and $CD14^{-}CD16^{+}$ monocyte subset has the lowest DR5 expression compared to others. The results is in line with the literature that monocytes mainly express DR4 and DR5 and also DR5 expression is usually higher than DR4 except in tissue-resident macrophages (Liguori et al., 2016; Washburn et al., 2003). Although, nonfunctional TRAIL-Rs, TRAIL-R3 and TRAIL-R4, could not be detected at protein level in two studies (Liguori et al., 2016; Washburn et al., 2003), one study which detects their expression at only gene level by qPCR (Griffith et al., 1999).

5.2. Susceptibility of primary human monocytes to TRAIL-induced cell death

Although TRAIL is known as an apoptosis inducer only in neoplastic cells, the expression of functional transmembrane TRAIL receptors on monocytes prompted the analysis of the susceptibility of primary human monocytes to rhTRAIL during differentiation to macrophages. As seen in **Figure 5**, the cell viability of TRAIL-treated monocytes was nearly the same as the control monocytes that were only cultured with M-CSF and the difference between them was not significant, indicating there is no difference in cell viability between experimental group and control group.

There is one study claiming that the viability of TRAIL-treated primary human monocytes decreases in a time-dependent manner that their survival is reduced to 50% after 72 hours of treatment (Liguori et al., 2016). The two conditions in our study is different than this study are that one is the type of recombinant TRAIL and the other one is the presence of M-CSF during treatment. SuperKiller TRAIL protein was used in that study and this recombinant TRAIL has an extra disulfide bridge so it increases the stability of the protein to effectively clustering on cell surface receptors. This formulation could increase the sensitivity of TRAIL-mediated apoptosis by either increasing the stability of the TRAIL or the affinity of TRAIL to the receptors. The other subject is the presence of M-CSF in our study which is extensively studied on monocytes and this polyfunctional factor is related to increased cell survival and/or proliferation, differentiation and activation in both monocytes and macrophages (Pixley & Stanley, 2004; Stanley et al., 1978). Therefore, no significant cytotoxicity was seen in our study after 7 days of incubation with rhTRAIL due to the distinct formulation of TRAIL and the presence very potent survival signal.

Moreover, to prevent uncontrolled cell death, expressing high levels of any of the cellular FLICE inhibitory protein (c-FLIP) known as procaspase-8 homolog, X-linked inhibitor of apoptosis (XIAP) and anti-apoptotic Bcl family proteins makes monocytes resistant to TRAIL-induced apoptosis (Vogler et al., 2007; Fulda et al., 2002; Irmler et al., 1997). In the literature, the time when immune cells become susceptible to TRAIL-mediated apoptosis is in the resolution phase of an immune response to prevent tissue damage and control the immune response (McGrath et al., 2011). Because of that, TRAIL might not induce cytotoxicity in monocytes that are not activated or senescent. In line with our results, it was reported that TRAIL did not induce cytotoxicity in THP-1 cell line (Wei et al., 2010; Secchiero et al., 2002).

5.3. The inter- and intra- group variability of control and TRAIL-treated macrophages

After showing that TRAIL does not initiate apoptosis on monocytes/macrophages during differentiation, RNA-sequencing was employed to uncover whether TRAIL treatment during monocyte to macrophage differentiation cause any changes in the transcriptome of both M0 macrophages and M1 macrophages. In the PCA plot (**Figure 7**), M0 macrophages and M1 macrophages are clustered with their own group. There is a clear separation between M0 and M1 macrophages based on PC1 and a slight difference between the TRAIL-treated group and the control group. This PCA plot suggests that macrophage polarization causes more variations in gene expression profile compared to TRAIL stimulation. These plots were created by using 3 different biological replicates and it is obvious that one of the donors is distinct from the other two donors based on the PC2 axis. The reason for this separation would be donor-dependent variations and lack of batch correction.

Spearman's correlation heat map indicated a similar conclusion. M0 and M1 groups are positively correlated by around 0.7 which is a strong correlation. The size of the square between M0 and M1 groups is relatively small compared to the treatment group. The size and color of the squares of the treatment group are quite similar to the ones in that the samples matching themselves. These findings indicate the same conclusion as the PCA plot that polarization causes more variations. The correlation range from 0.7 to 1.0 is consistent with each group sharing a common origin and this is reasonable M1 macrophages arise from M0 macrophages with certain stimuli.

5.4. The analysis of DEGs in M0 and M1 groups by qPCR and ELISA

The next step was the analysis of differentially expressed genes between the TRAIL-treated group versus the control group to further explore the transcriptional changes after TRAIL stimulation. The combination of false discovery rate (FDR) and fold-change (FC) in logarithmic scale (base 2) was used to select DEGs in RNA-seq data analysis in terms of reproducibility and decreased false-positive rate. Sorted RNA-seq data uncovered 29 transcripts of the TM1 vs M1 group and 8 transcripts of the TM0 and M0 groups. For the downstream analysis, CXCL11, LILRA5, HGF and PACERR were selected for the M1 group while CXCL9, CXCL8, and CXCL5 were selected for the M0 group. TNF was also selected for both M0 and M1 groups even if it was not significant in the RNA-seq data.

CXCL11, referred to as the interferon-inducible T-cell alpha chemoattractant(I-TAC) or interferon-gamma-inducible protein 9 (IP9) is a small chemokine that play role in the regulation of immune cell migration such as activated T cells, activation and differentiation of cells (Torraca et al., 2015). It is highly expressed by M1 macrophages due to its expression strongly induced by IFN-γ (Cao et al., 2021). LILRA5, leukocyte immunoglobulin-like receptor A5, mostly expressed by monocytes and neutrophils and activation on monocytes promotes the production of pro-inflammatory cytokines such as TNF, IL-1ß and IL-6 (Brown et al., 2004; Borges et al., 2003). The qPCR results of LILRA5 and CXCL11 did not have the same trend as the RNA-seq data and their expression was lower than the control group. Previously it was shown that the expression of LILRA5 at the mRNA level in freshly isolated primary monocytes was down-regulated after short-term culture (12h) with TNF but the level of soluble LILRA5 protein was increased in cell supernatant (Mitchell et al., 2008). Since TRAIL is a member of TNF family, TRAIL may also regulate LILRA5 expression as the same way TNF does by enhancing cell surface cleavage.

Although CXCL11 mRNA expression was reduced in TRAIL-treated M1 macrophages compared to the control group, CXCL11 secretion, in contrast, was enhanced in the same group. The posttranscriptional mechanism responsible for this discrepancy in CXCL11 regulation between mRNA and protein levels has to be further investigated.

Hepatocyte growth factor (HGF) is a multifunctional protein that plays important roles in the regeneration process of various tissues and the migration of respective progenitor cells. It is well-known that M2 macrophages produce an abundant level of HGF and also HGF promotes macrophage transition to the M2 phenotype (Nishikoba et al., 2020; Choi et al., 2019). Although M1 macrophages already express low levels of HGF, our data showed that the TRAIL treatment significantly decreased the expression of HGF, suggesting that TRAIL might further inhibit HGF/c-Met signaling. PACERR/PACER is an antisense lncRNA, accelerating COX-2 expression by increasing chromatin accessibility (Krawczyk & Emerson, 2014). A large body of studies describes a link between COX-2 and macrophage polarization to M2 phenotype (Wang et al., 2017; Li et al., 2015; Na et al., 2013; Nakanishi et al., 2011). It was reported that the transcription initiation of COX-2 was significantly decreased upon PACERR knockdown so that the downregulation of PACERR in M1 macrophages could further attenuate the expression of COX-2 and its products (Krawczyk & Emerson, 2014).

In the M0 group, CXCL9 is one of the M1 macrophage marker because its expression in macrophages inhibited by IL-4 and IL-10 which are potent stimuli for M2 macrophage (Mantovani et al., 2002). The expression of CXCL9 was enhanced while the expression CXCL8 and CXCL5 was decreased in TRAIL-treated M1 macrophages. CXCL8 and CXCL5 were reported to play roles in the progression of various cancers including breast cancer, colorectal cancer, non-small cell lung cancer, gastric cancer and melanoma. In contrast, CXCL9 is known to be associated with tumor regression and increased survival, possibly because of increasing infiltrating of leukocytes and dendritic cells (Zhu et al., 2020; Hosono et al., 2017; Liu et al., 2016; Richmond, 2002).

TNF is a pleiotropic cytokine that is involved in multiple hemostatic and pathological conditions and M1 macrophages are the major source of this cytokine (Laha et al., 2021; Lu et al., 2018). This prominent marker of M1 macrophages was also selected for qPCR analysis even if TNF expression was not significantly different in TRAIL-treated M1 and M0 macrophages analyzed by RNA-seq. Nonetheless, TRAIL-treated M1 macrophages demonstrated a significant increase in TNF expression at both mRNA and protein levels. mRNA expression of TNF was also significantly enhanced in TRAIL-treated M0 macrophages (**Figure 11.C and Figure 12.E**). Similar results were reported that the mRNA expression of TNF was significantly increased in human-monocyte-derived macrophages treated with recombinant soluble TRAIL. Also, the mRNA expression and the serum level of TNF was also increased in peritoneal macrophages of mice in response to recombinant soluble TRAIL treatment (Gao et al., 2015). Together with the literature, TRAIL possesses a pro-inflammatory ability in both unpolarized macrophages and M1 macrophages *in vitro*.

In summary, these findings provide novel insights into immunoregulatory functions of TRAIL signaling in the differentiation of primary human monocytes to macrophages through either efficient suppression of anti-inflammatory mediators or induction of the pro-inflammatory mediators. Most importantly, this study offers a valuable background for further studies of the immunomodulatory role of TRAIL in monocyte differentiation and M1 macrophage response.

6. Conclusion

To sum up, the findings of this study suggest that TRAIL-stimulated macrophages exert a pro-inflammatory phenotype, indicating that TRAIL stimulation shifts M0 macrophages towards an M1 phenotype, while TRAIL-treated macrophages synergizes with LPS and IFN-γ in enhancing the pro-inflammatory ability of M1 macrophages, *in vitro*. It is particularly remarkable that the immunoregulatory activity of TRAIL in primary human monocytes without any cytotoxicity demonstrates that TRAIL is a potent inducer for pro-inflammatory phenotype for both monocytes and macrophages.

In addition to this, TRAIL stimulation in both M0 and M1 macrophages down-regulated M2-related markers including HGF, PACERR, CXCL8 and CXCL5. This indicates that TRAIL is negatively associated with the production of M2- related factors. To determine whether TRAIL stimulation attenuates well-known M2 markers, the surface expression of CD163, CD206 and secretion of IL-10, TGF-ß and VEGF could be checked in M2 macrophages.

The other aspect to be considered is how monocytes or macrophages are resistant to TRAIL-mediated apoptosis. The expression of decoy receptors on monocytes is still obscure since these receptors lack death domain so they can not initiate apoptosis. Besides, the concentration of anti-apoptotic proteins such as c-FLIP, XIAP, and Bcl family proteins could be investigated since high expression of these proteins can inhibit the initiation of apoptosis. Downstream mechanisms of TRAIL receptors which are responsible for the switch between apoptotic and non-apoptotic pathways in monocytes and macrophages should be further investigated.

Taking everything into account, our study sheds light on the regulation of monocyte differentiation and M1 polarization by TRAIL *in vitro* and suggests that TRAIL is a potential mediator of macrophage polarization.

7. References

Abbott, M., and Ustoyev, Y. (2019). Cancer and the Immune System: The History and Background of Immunotherapy. Seminars in Oncology Nursing, 35(5), 150923. https://doi.org/10.1016/j.soncn.2019.08.002

Abumaree, M. H., Al Jumah, M. A., Kalionis, B., Jawdat, D., Al Khaldi, A., Abomaray, F. M., … Knawy, B. A. (2013). Human Placental Mesenchymal Stem Cells (pMSCs) Play a Role as Immune Suppressive Cells by Shifting Macrophage Differentiation from Inflammatory M1 to Anti-inflammatory M2 Macrophages. Stem Cell Reviews and Reports, 9(5), 620-641. https://doi.org/10.1007/s12015-013-9455-2

Ancuta, P., Rao, R., Moses, A., Mehle, A., Shaw, S. K., Luscinskas, F. W., and Gabuzda, D. (2003). Fractalkine Preferentially Mediates Arrest and Migration of CD16+ Monocytes. Journal of Experimental Medicine, 197(12), 1701-1707. https://doi.org/10.1084/jem.20022156

Ashkenazi, A., Pai, R. C., Fong, S., Leung, S., Lawrence, D. A., Marsters, S. A., … Schwall, R. H. (1999). Safety and antitumor activity of recombinant soluble Apo2 ligand. The Journal of Clinical Investigation, 104(2), 155–162. https://doi.org/10.1172/JCI6926

Barros, M. H. M., Hauck, F., Dreyer, J. H., Kempkes, B., and Niedobitek, G. (2013). Macrophage Polarisation: An Immunohistochemical Approach for Identifying M1 and M2 Macrophages. PLoS ONE, 8(11), e80908. https://doi.org/10.1371/journal.pone.0080908

Biswas, S. K., and Mantovani, A. (2012). Orchestration of metabolism by macrophages. Cell Metabolism, 15(4), 432–437. https://doi.org/10.1016/j.cmet.2011.11.013

Bodmer, J. L., Holler, N., Reynard, S., Vinciguerra, P., Schneider, P., Juo, P., … Tschopp, J. (2000). TRAIL receptor-2 signals apoptosis through FADD and caspase-8. Nature Cell Biology, 2(4), 241-243. https://doi.org/10.1038/35008667

Bonilla, F. A., and Oettgen, H. C. (2010). Adaptive immunity. Journal of Allergy and Clinical Immunology, 125(2), S33–S40. https://doi.org/10.1016/j.jaci.2009.09.017

Borges, L., Kubin, M., and Kuhlman, T. (2003). LIR9, an immunoglobulin-superfamily-activating receptor, is expressed as a transmembrane and as a secreted molecule. Blood, 101(4), 1484–1486. https://doi.org/10.1182/blood-2002-05-1432

Boyette, L. B., Macedo, C., Hadi, K., Elinoff, B. D., Walters, J. T., Ramaswami, B., … Metes, D. M. (2017). Phenotype, function, and differentiation potential of human monocyte subsets. PloS One, 12(4), e0176460. https://doi.org/10.1371/journal.pone.0176460

Bozec, A., and Soulat, D. (2017). Latest perspectives on macrophages in bone homeostasis. Pflügers Archiv - European Journal of Physiology, 469(3), 517–525. https://doi.org/10.1007/s00424-017-1952-8

Brown, D., Trowsdale, J., and Allen, R. (2004). The LILR family: Modulators of innate and adaptive immune pathways in health and disease. Tissue Antigens, 64(3), 215–225. https://doi.org/10.1111/j.0001-2815.2004.00290.x

Buracchi, C., Pasqualini, F., Bergomas, F., Pesce, S., Sironi, M., Grizzi, F., … Allavena, P. (2016). Functional TRAIL receptors in monocytes and tumor-associated macrophages: A possible targeting pathway in the tumor microenvironment. Oncotarget. https://doi.org/10.18632/oncotarget.9340

Canton, J., Neculai, D., and Grinstein, S. (2013). Scavenger receptors in homeostasis and immunity. Nature Reviews. Immunology, 13(9), 621–634. https://doi.org/10.1038/nri3515

Cao, Y., Jiao, N., Sun, T., Ma, Y., Zhang, X., Chen, H., … Zhang, Y. (2021). CXCL11 Correlates With Antitumor Immunity and an Improved Prognosis in Colon Cancer. Frontiers in Cell and Developmental Biology, 9. Retrieved from https://www.frontiersin.org/articles/10.3389/fcell.2021.646252

Cardoso Alves, L., Berger, M. D., Koutsandreas, T., Kirschke, N., Lauer, C., Spörri, R., … Krebs, P. (2020). Non-apoptotic TRAIL function modulates NK cell activity during viral infection. EMBO Reports, 21(1), e48789. https://doi.org/10.15252/embr.201948789

Chan, J., Prado-Lourenco, L., Khachigian, L. M., Bennett, M. R., Di Bartolo, B. A., and Kavurma, M. M. (2010). TRAIL Promotes VSMC Proliferation and Neointima Formation in a FGF-2-, Sp1 Phosphorylation-, and NFκB-Dependent Manner. Circulation Research, 106(6), 1061–1071. https://doi.org/10.1161/CIRCRESAHA.109.206029

Chaudhary, P. M., Eby, M., Jasmin, A., Bookwalter, A., Murray, J., and Hood, L. (1997). Death receptor 5, a new member of the TNFR family, and DR4 induce FADD-dependent apoptosis and activate the NF-kappaB pathway. Immunity, 7(6), 821-830. https://doi.org/10.1016/s1074-7613(00)80400-8

Choi, W., Lee, J., Lee, J., Lee, S. H., and Kim, S. (2019). Hepatocyte Growth Factor Regulates Macrophage Transition to the M2 Phenotype and Promotes Murine Skeletal Muscle Regeneration. Frontiers in Physiology, 10, 914. https://doi.org/10.3389/fphys.2019.00914

Chyuan, I.-T., Tsai, H.-F., Liao, H.-J., Wu, C.-S., and Hsu, P.-N. (2018). An apoptosis-independent role of TRAIL in suppressing joint inflammation and inhibiting T-cell activation in inflammatory arthritis. Cellular & Molecular Immunology, 15(9), 846-857. https://doi.org/10.1038/cmi.2017.2

Cole, K. E., Strick, C. A., Paradis, T. J., Ogborne, K. T., Loetscher, M., Gladue, R. P., … Neote, K. (1998). Interferon–inducible T Cell Alpha Chemoattractant (I-TAC): A Novel Non-ELR CXC Chemokine with Potent Activity on Activated T Cells through Selective High Affinity Binding to CXCR3. The Journal of Experimental Medicine, 187(12), 2009–2021. Retrieved from https://www.ncbi.nlm.nih.gov/pmc/articles/PMC2212354/

de Gaetano, M., Crean, D., Barry, M., and Belton, O. (2016). M1- and M2-Type Macrophage Responses Are Predictive of Adverse Outcomes in Human Atherosclerosis. Frontiers in Immunology, 7. https://doi.org/10.3389/fimmu.2016.00275

Degli-Esposti, M. A., Dougall, W. C., Smolak, P. J., Waugh, J. Y., Smith, C. A., and Goodwin, R. G. (1997). The novel receptor TRAIL-R4 induces NF-kappaB and protects against TRAIL-mediated apoptosis, yet retains an incomplete death domain. Immunity, 7(6), 813–820. https://doi.org/10.1016/s1074-7613(00)80399-4

Dong, N., Shi, X., Wang, S., Gao, Y., Kuang, Z., Xie, Q., ... Li, J.-L. (2019). M2 macrophages mediate sorafenib resistance by secreting HGF in a feed-forward manner in hepatocellular carcinoma. British Journal of Cancer, 121(1), 22–33. https://doi.org/10.1038/s41416-019-0482-x

Dongre, A., and Weinberg, R. A. (2019). New insights into the mechanisms of epithelial–mesenchymal transition and implications for cancer. Nature Reviews Molecular Cell Biology, 20(2), 69–84. https://doi.org/10.1038/s41580-018-0080-4

Duluc, D., Delneste, Y., Tan, F., Moles, M.-P., Grimaud, L., Lenoir, J., ... Jeannin, P. (2007). Tumor-associated leukemia inhibitory factor and IL-6 skew monocyte differentiation into tumor-associated macrophage-like cells. Blood, 110(13), 4319–4330. https://doi.org/10.1182/blood-2007-02-072587

Dunkelberger, J. R., and Song, W.-C. (2010). Complement and its role in innate and adaptive immune responses. Cell Research, 20(1), 34–50. https://doi.org/10.1038/cr.2009.139

Epelman, S., Lavine, K. J., and Randolph, G. J. (2014). Origin and Functions of Tissue Macrophages. Immunity, 41(1), 21–35. https://doi.org/10.1016/j.immuni.2014.06.013

Farber, D. L., Netea, M. G., Radbruch, A., Rajewsky, K., and Zinkernagel, R. M. (2016). Immunological memory: Lessons from the past and a look to the future. Nature Reviews Immunology, 16(2), 124–128. https://doi.org/10.1038/nri.2016.13

Ferrante, C. J., Pinhal-Enfield, G., Elson, G., Cronstein, B. N., Hasko, G., Outram, S., and Leibovich, S. J. (2013). The Adenosine-Dependent Angiogenic Switch of Macrophages to an M2-Like Phenotype is Independent of Interleukin-4 Receptor Alpha (IL-4Rα) Signaling. Inflammation, 36(4), 921–931. https://doi.org/10.1007/s10753-013-9621-3

Franco, A. V., Zhang, X. D., Van Berkel, E., Sanders, J. E., Zhang, X. Y., Thomas, W. D., ... Hersey, P. (2001). The role of NF-kappa B in TNF-related apoptosis-inducing ligand (TRAIL)-induced apoptosis of melanoma cells. Journal of Immunology (Baltimore, Md.: 1950), 166(9), 5337-5345. https://doi.org/10.4049/jimmunol.166.9.5337

Fulda, S., Meyer, E., and Debatin, K.-M. (2002). Inhibition of TRAIL-induced apoptosis by Bcl-2 overexpression. Oncogene, 21(15), 2283–2294. https://doi.org/10.1038/sj.onc.1205258

Gao, J., Wang, D., Liu, D., Liu, M., Ge, Y., Jiang, M., … Zheng, D. (2015). Tumor necrosis factor-related apoptosis-inducing ligand induces the expression of proinflammatory cytokines in macrophages and re-educates tumor-associated macrophages to an antitumor phenotype. Molecular Biology of the Cell, 26(18), 3178–3189. https://doi.org/10.1091/mbc.e15-04-0209

Gasteiger, G., D'Osualdo, A., Schubert, D. A., Weber, A., Bruscia, E. M., and Hartl, D. (2017). Cellular Innate Immunity: An Old Game with New Players. Journal of Innate Immunity, 9(2), 111-125. https://doi.org/10.1159/000453397

Gaudino, S. J., and Kumar, P. (2019). Cross-Talk Between Antigen Presenting Cells and T Cells Impacts Intestinal Homeostasis, Bacterial Infections, and Tumorigenesis. Frontiers in Immunology, 10. Retrieved from https://www.frontiersin.org/articles/10.3389/fimmu.2019.00360

Gautier, E. L., Shay, T., Miller, J., Greter, M., Jakubzick, C., Ivanov, S., … Immunological Genome Consortium. (2012). Gene-expression profiles and transcriptional regulatory pathways that underlie the identity and diversity of mouse tissue macrophages. Nature Immunology, 13(11), 1118-1128. https://doi.org/10.1038/ni.2419

Gerhardt, T., and Ley, K. (2015). Monocyte trafficking across the vessel wall. Cardiovascular Research, 107(3), 321-330. https://doi.org/10.1093/cvr/cvv147

Ghousifam, N., Eftekharjoo, M., Derakhshan, T., and Gappa-Fahlenkamp, H. (2019, March 14). Effects of Local Concentration Gradients of Monocyte Chemoattractant Protein-1 (MCP-1) on Monocytes Adhesion and Transendothelial Migration in a Three-Dimensional (3D) In Vitro Vascular Tissue Model. arXiv. https://doi.org/10.48550/arXiv.1903.05144

Gordon, R. A., Grigoriev, G., Lee, A., Kalliolias, G. D., and Ivashkiv, L. B. (2012). The interferon signature and STAT1 expression in rheumatoid arthritis synovial fluid macrophages are induced by tumor necrosis factor α and counter-regulated by the synovial fluid microenvironment. Arthritis and Rheumatism, 64(10), 3119-3128. https://doi.org/10.1002/art.34544

Gordon, S., and Martinez, F. O. (2010). Alternative Activation of Macrophages: Mechanism and Functions. Immunity, 32(5), 593-604. https://doi.org/10.1016/j.immuni.2010.05.007

Griffith, T. S., Wiley, S. R., Kubin, M. Z., Sedger, L. M., Maliszewski, C. R., and Fanger, N. A. (1999). Monocyte-mediated Tumoricidal Activity via the Tumor Necrosis Factor-related Cytokine, TRAIL. The Journal of Experimental Medicine, 189(8), 1343-1354. Retrieved from https://www.ncbi.nlm.nih.gov/pmc/articles/PMC2193036/

Gschwandtner, M., Derler, R., and Midwood, K. S. (2019). More Than Just Attractive: How CCL2 Influences Myeloid Cell Behavior Beyond Chemotaxis. Frontiers in Immunology, 10. Retrieved from https://www.frontiersin.org/articles/10.3389/fimmu.2019.02759

GTEx Consortium. (2013). The Genotype-Tissue Expression (GTEx) project. Nature Genetics, 45(6), 580-585. https://doi.org/10.1038/ng.2653

Hao, S., Meng, J., Zhang, Y., Liu, J., Nie, X., Wu, F., … Xu, H. (2017). Macrophage phenotypic mechanomodulation of enhancing bone regeneration by superparamagnetic scaffold upon magnetization. Biomaterials, 140, 16-25. https://doi.org/10.1016/j.biomaterials.2017.06.013

Hardy, L. A., Booth, T. A., Lau, E. K., Handel, T. M., Ali, S., and Kirby, J. A. (2004). Examination of MCP-1 (CCL2) partitioning and presentation during transendothelial leukocyte migration. Laboratory Investigation, 84(1), 81-90. https://doi.org/10.1038/labinvest.3700007

Henson, P. M., and Hume, D. A. (2006). Apoptotic cell removal in development and tissue homeostasis. Trends in Immunology, 27(5), 244-250. https://doi.org/10.1016/j.it.2006.03.005

Hilliard, B., Wilmen, A., Seidel, C., Liu, T. S., Göke, R., and Chen, Y. (2001). Roles of TNF-related apoptosis-inducing ligand in experimental autoimmune encephalomyelitis. Journal of Immunology (Baltimore, Md.: 1950), 166(2), 1314–1319. https://doi.org/10.4049/jimmunol.166.2.1314

Holen, I., Croucher, P. I., Hamdy, F. C., and Eaton, C. L. (2002). Osteoprotegerin (OPG) is a survival factor for human prostate cancer cells. Cancer Research, 62(6), 1619–1623.

Hosono, M., Koma, Y.-I., Takase, N., Urakawa, N., Higashino, N., Suemune, K., … Yokozaki, H. (2017). CXCL8 derived from tumor-associated macrophages and esophageal squamous cell carcinomas contributes to tumor progression by promoting migration and invasion of cancer cells. Oncotarget, 8(62), 106071-106088. https://doi.org/10.18632/oncotarget.22526

Ikeda, T., Hirata, S., Fukushima, S., Matsunaga, Y., Ito, T., Uchino, M., … Senju, S. (2010). Dual Effects of TRAIL in Suppression of Autoimmunity: The Inhibition of Th1 Cells and the Promotion of Regulatory T Cells. The Journal of Immunology, 185(9), 5259–5267. https://doi.org/10.4049/jimmunol.0902797

Irmler, M., Thome, M., Hahne, M., Schneider, P., Hofmann, K., Steiner, V., … Tschopp, J. (1997). Inhibition of death receptor signals by cellular FLIP. Nature, 388(6638), 190–195. https://doi.org/10.1038/40657

Italiani, P., and Boraschi, D. (2014). From Monocytes to M1/M2 Macrophages: Phenotypical vs. Functional Differentiation. Frontiers in Immunology, 5. Retrieved from https://www.frontiersin.org/articles/10.3389/fimmu.2014.00514

Jiang, Y., Chen, X., Fan, M., Li, H., Zhu, W., Chen, X., … Ma, Y. (2017). TRAIL facilitates cytokine expression and macrophage migration during hypoxia/reoxygenation via ER stress-dependent NF-κB pathway. Molecular Immunology, 82, 123–136. https://doi.org/10.1016/j.molimm.2016.12.023

Jiang, Z., Jiang, J. X., and Zhang, G.-X. (2014). Macrophages: A double-edged sword in experimental autoimmune encephalomyelitis. Immunology Letters, 160(1), 17-22. https://doi.org/10.1016/j.imlet.2014.03.006

Kavurma, M. M., Schoppet, M., Bobryshev, Y. V., Khachigian, L. M., and Bennett, M. R. (2008). TRAIL stimulates proliferation of vascular smooth muscle cells via activation of NF-kappaB and induction of insulin-like growth factor-1 receptor. The Journal of Biological Chemistry, 283(12), 7754–7762. https://doi.org/10.1074/jbc.M706927200

Kawai, T., and Akira, S. (2010). The role of pattern-recognition receptors in innate immunity: Update on Toll-like receptors. Nature Immunology, 11(5), 373–384. https://doi.org/10.1038/ni.1863

Kischkel, F. C., Lawrence, D. A., Tinel, A., LeBlanc, H., Virmani, A., Schow, P., ... Ashkenazi, A. (2001). Death receptor recruitment of endogenous caspase-10 and apoptosis initiation in the absence of caspase-8. The Journal of Biological Chemistry, 276(49), 46639–46646. https://doi.org/10.1074/jbc.M105102200

Kohyama, M., Ise, W., Edelson, B. T., Wilker, P. R., Hildner, K., Mejia, C., … Murphy, K. M. (2009). Role for Spi-C in the development of red pulp macrophages and splenic iron homeostasis. Nature, 457(7227), 318–321. https://doi.org/10.1038/nature07472

Korkosz, M., Bukowska-Strakova, K., Sadis, S., Grodzicki, T., and Siedlar, M. (2012). Monoclonal antibodies against macrophage colony-stimulating factor diminish the number of circulating intermediate and nonclassical (CD14(++)CD16(+)/CD14(+)CD16(++)) monocytes in rheumatoid arthritis patient. Blood, 119(22), 5329–5330. https://doi.org/10.1182/blood-2012-02-412551

Krawczyk, M., and Emerson, B. M. (2014). P50-associated COX-2 extragenic RNA (PACER) activates COX-2 gene expression by occluding repressive NF-κB complexes. ELife, 3, e01776. https://doi.org/10.7554/eLife.01776

Kurowska-Stolarska, M., Stolarski, B., Kewin, P., Murphy, G., Corrigan, C. J., Ying, S., ... Liew, F. Y. (2009). IL-33 amplifies the polarization of alternatively activated macrophages that contribute to airway inflammation. Journal of Immunology (Baltimore, Md.: 1950), 183(10), 6469–6477. https://doi.org/10.4049/jimmunol.0901575

Laha, D., Grant, R., Mishra, P., and Nilubol, N. (2021). The Role of Tumor Necrosis Factor in Manipulating the Immunological Response of Tumor Microenvironment. Frontiers in Immunology, 12. Retrieved from https://www.frontiersin.org/articles/10.3389/fimmu.2021.656908

LeBlanc, H. N., and Ashkenazi, A. (2003). Apo2L/TRAIL and its death and decoy receptors. Cell Death & Differentiation, 10(1), 66–75. https://doi.org/10.1038/sj.cdd.4401187

Li, H., Zhu, H., Xu, C. J., and Yuan, J. (1998). Cleavage of BID by caspase 8 mediates the mitochondrial damage in the Fas pathway of apoptosis. Cell, 94(4), 491-501. https://doi.org/10.1016/s0092-8674(00)81590-1

Li, Hongzhong, Yang, B., Huang, J., Lin, Y., Xiang, T., Wan, J., … Ren, G. (2015). Cyclooxygenase-2 in tumor-associated macrophages promotes breast cancer cell survival by triggering a positive-feedback loop between macrophages and cancer cells. Oncotarget, 6(30), 29637–29650. Retrieved from https://www.ncbi.nlm.nih.gov/pmc/articles/PMC4745752/

Li, Y., Xie, Z., Wang, Y., and Hu, H. (2018). Macrophage M1/M2 polarization in patients with pregnancy-induced hypertension. Canadian Journal of Physiology and Pharmacology, 96(9), 922–928. https://doi.org/10.1139/cjpp-2017-0694

Liao, X., Sharma, N., Kapadia, F., Zhou, G., Lu, Y., Hong, H., … Jain, M. K. (2011). Krüppel-like factor 4 regulates macrophage polarization. The Journal of Clinical Investigation, 121(7), 2736–2749. https://doi.org/10.1172/JCI45444

Liguori, M., Buracchi, C., Pasqualini, F., Bergomas, F., Pesce, S., Sironi, M., … Allavena, P. (2106). Functional TRAIL receptors in monocytes and tumor-associated macrophages: A possible targeting pathway in the tumor microenvironment. Oncotarget, 7(27), 41662–41676. https://doi.org/10.18632/oncotarget.9340

Lin, Y., Devin, A., Cook, A., Keane, M. M., Kelliher, M., Lipkowitz, S., and Liu, Z. G. (2000). The death domain kinase RIP is essential for TRAIL (Apo2L)-induced activation of IkappaB kinase and c-Jun N-terminal kinase. Molecular and Cellular Biology, 20(18), 6638–6645. https://doi.org/10.1128/MCB.20.18.6638-6645.2000

Liu, J., Geng, X., Hou, J., and Wu, G. (2021). New insights into M1/M2 macrophages: Key modulators in cancer progression. Cancer Cell International, 21(1), 389. https://doi.org/10.1186/s12935-021-02089-2

Liu, Q., Li, A., Tian, Y., Wu, J. D., Liu, Y., Li, T., … Wu, K. (2016). The CXCL8-CXCR1/2 pathways in cancer. Cytokine & Growth Factor Reviews, 31, 61–71. https://doi.org/10.1016/j.cytogfr.2016.08.002

Lu, H.-L., Huang, X.-Y., Luo, Y.-F., Tan, W.-P., Chen, P.-F., and Guo, Y.-B. (2018). Activation of M1 macrophages plays a critical role in the initiation of acute lung injury. Bioscience Reports, 38(2), BSR20171555. https://doi.org/10.1042/BSR20171555

Lu, T., Ramakrishnan, R., Altiok, S., Youn, J.-I., Cheng, P., Celis, E., … Gabrilovich, D. (2011). Tumor-infiltrating myeloid cells induce tumor cell resistance to cytotoxic T cells in mice. The Journal of Clinical Investigation, 121(10), 4015–4029. https://doi.org/10.1172/JCI45862

Mantovani, A., Allavena, P., Sica, A., and Balkwill, F. (2008). Cancer-related inflammation. Nature, 454(7203), 436–444. https://doi.org/10.1038/nature07205

Mantovani, A., Sica, A., Sozzani, S., Allavena, P., Vecchi, A., and Locati, M. (2004). The chemokine system in diverse forms of macrophage activation and polarization. Trends in Immunology, 25(12), 677–686. https://doi.org/10.1016/j.it.2004.09.015

Mantovani, A., Sozzani, S., Locati, M., Allavena, P., and Sica, A. (2002). Macrophage polarization: Tumor-associated macrophages as a paradigm for polarized M2 mononuclear phagocytes. Trends in Immunology, 23(11), 549–555. https://doi.org/10.1016/s1471-4906(02)02302-5

Marshall, J. S., Warrington, R., Watson, W., and Kim, H. L. (2018). An introduction to immunology and immunopathology. Allergy, Asthma & Clinical Immunology, 14(S2), 49. https://doi.org/10.1186/s13223-018-0278-1

Martinez, F. O., and Gordon, S. (2014). The M1 and M2 paradigm of macrophage activation: Time for reassessment. F1000Prime Reports, 6, 13. https://doi.org/10.12703/P6-13

Mauro, A., Russo, V., Di Marcantonio, L., Berardinelli, P., Martelli, A., Muttini, A., … Barboni, B. (2016). M1 and M2 macrophage recruitment during tendon regeneration induced by amniotic epithelial cell allotransplantation in ovine. Research in Veterinary Science, 105, 92–102. https://doi.org/10.1016/j.rvsc.2016.01.014

McDermaid, A., Monier, B., Zhao, J., Liu, B., and Ma, Q. (2018). Interpretation of differential gene expression results of RNA-seq data: Review and integration. Briefings in Bioinformatics, 20(6), 2044–2054. https://doi.org/10.1093/bib/bby067

McGrath, E. E., Marriott, H. M., Lawrie, A., Francis, S. E., Sabroe, I., Renshaw, S. A., … Whyte, M. K. B. (2011). TNF-related apoptosis-inducing ligand (TRAIL) regulates inflammatory neutrophil apoptosis and enhances resolution of inflammation. Journal of Leukocyte Biology, 90(5), 855–865. https://doi.org/10.1189/jlb.0211062

Medzhitov, R., and Janeway, C. A. (1997). Innate Immunity: The Virtues of a Nonclonal System of Recognition. Cell, 91(3), 295–298. https://doi.org/10.1016/S0092-8674(00)80412-2

Medzhitov, R., and Janeway, CharleS. J. (2000). Innate immune recognition: Mechanisms and pathways: Innate immune recognition. Immunological Reviews, 173(1), 89–97. https://doi.org/10.1034/j.1600-065X.2000.917309.x

Mitchell, A., Rentero, C., Endoh, Y., Hsu, K., Gaus, K., Geczy, C., … Tedla, N. (2008). LILRA5 is expressed by synovial tissue macrophages in rheumatoid arthritis, selectively induces pro-inflammatory cytokines and IL-10 and is regulated by TNF-α, IL-10 and IFN-γ. European Journal of Immunology, 38(12), 3459–3473. https://doi.org/10.1002/eji.200838415

Miyanaka, Y., Ueno, Y., Tanaka, S., Yoshioka, K., Hatakeyama, T., Shimamoto, M., … Chayama, K. (2007). Clinical significance of mucosal suppressors of cytokine signaling 3 expression in ulcerative colitis. World Journal of Gastroenterology: WJG, 13(21), 2939–2944. https://doi.org/10.3748/wjg.v13.i21.2939

Morel, J., Audo, R., Hahne, M., and Combe, B. (2005). Tumor necrosis factor-related apoptosis-inducing ligand (TRAIL) induces rheumatoid arthritis synovial fibroblast proliferation through mitogen-activated protein kinases and phosphatidylinositol 3-kinase/Akt. The Journal of Biological Chemistry, 280(16), 15709–15718. https://doi.org/10.1074/jbc.M414469200

Mosser, D. M., Hamidzadeh, K., and Goncalves, R. (2021). Macrophages and the maintenance of homeostasis. Cellular & Molecular Immunology, 18(3), 579–587. https://doi.org/10.1038/s41423-020-00541-3

Mulder, R., Banete, A., and Basta, S. (2014). Spleen-derived macrophages are readily polarized into classically activated (M1) or alternatively activated (M2) states. Immunobiology, 219(10), 737–745. https://doi.org/10.1016/j.imbio.2014.05.005

Murphy, K. M., and Weaver, C. (2017). Janeway's Immunobiology. Garland Science/Taylor & Francis Group, LLC.

Murray, P. J. (2017). Macrophage Polarization. Annual Review of Physiology, 79(1), 541–566. https://doi.org/10.1146/annurev-physiol-022516-034339

Na, Y.-R., Yoon, Y.-N., Son, D.-I., and Seok, S.-H. (2013). Cyclooxygenase-2 Inhibition Blocks M2 Macrophage Differentiation and Suppresses Metastasis in Murine Breast Cancer Model. PLoS ONE, 8(5), e63451. https://doi.org/10.1371/journal.pone.0063451

Nakanishi, Y., Nakatsuji, M., Seno, H., Ishizu, S., Akitake-Kawano, R., Kanda, K., … Chiba, T. (2011). COX-2 inhibition alters the phenotype of tumor-associated macrophages from M2 to M1 in ApcMin/+ mouse polyps. Carcinogenesis, 32(9), 1333–1339. https://doi.org/10.1093/carcin/bgr128

Netea, M. G., Balkwill, F., Chonchol, M., Cominelli, F., Donath, M. Y., Giamarellos-Bourboulis, E. J., … Dinarello, C. A. (2017). A guiding map for inflammation. Nature Immunology, 18(8), 826–831. https://doi.org/10.1038/ni.3790

Netea, M. G., Schlitzer, A., Placek, K., Joosten, L. A. B., and Schultze, J. L. (2019). Innate and Adaptive Immune Memory: An Evolutionary Continuum in the Host's Response to Pathogens. Cell Host & Microbe, 25(1), 13–26. https://doi.org/10.1016/j.chom.2018.12.006

Nishikoba, N., Kumagai, K., Kanmura, S., Nakamura, Y., Ono, M., Eguchi, H., … Ido, A. (2020). HGF-MET Signaling Shifts M1 Macrophages Toward an M2-Like Phenotype Through PI3K-Mediated Induction of Arginase-1 Expression. Frontiers in Immunology, 11. Retrieved from https://www.frontiersin.org/articles/10.3389/fimmu.2020.02135

Nobs, S. P., and Kopf, M. (2021). Tissue-resident macrophages: Guardians of organ homeostasis. Trends in Immunology, 42(6), 495–507. https://doi.org/10.1016/j.it.2021.04.007

Ozören, N., and El-Deiry, W. S. (2002). Defining characteristics of Types I and II apoptotic cells in response to TRAIL. Neoplasia (New York, N.Y.), 4(6), 551–557. https://doi.org/10.1038/sj.neo.7900270

Pan, Y., Yu, Y., Wang, X., and Zhang, T. (2020). Tumor-Associated Macrophages in Tumor Immunity. Frontiers in Immunology, 11, 583084. https://doi.org/10.3389/fimmu.2020.583084

Parkin, J., and Cohen, B. (2001). An overview of the immune system. The Lancet, 357(9270), 1777–1789. https://doi.org/10.1016/S0140-6736(00)04904-7

Passlick, B., Flieger, D., and Ziegler-Heitbrock, H. W. (1989). Identification and characterization of a novel monocyte subpopulation in human peripheral blood. Blood, 74(7), 2527–2534.

Perdiguero, E. G., and Geissmann, F. (2016). Development and maintainance of resident macrophages. Nature Immunology, 17(1), 2–8. https://doi.org/10.1038/ni.3341

Perry, V. H., Nicoll, J. A. R., and Holmes, C. (2010). Microglia in neurodegenerative disease. Nature Reviews. Neurology, 6(4), 193–201. https://doi.org/10.1038/nrneurol.2010.17

Pitti, R. M., Marsters, S. A., Ruppert, S., Donahue, C. J., Moore, A., and Ashkenazi, A. (1996). Induction of apoptosis by Apo-2 ligand, a new member of the tumor necrosis factor cytokine family. The Journal of Biological Chemistry, 271(22), 12687–12690. https://doi.org/10.1074/jbc.271.22.12687

Pixley, F. J., and Stanley, E. R. (2004). CSF-1 regulation of the wandering macrophage: Complexity in action. Trends in Cell Biology, 14(11), 628–638. https://doi.org/10.1016/j.tcb.2004.09.016

Poltavets, A. S., Vishnyakova, P. A., Elchaninov, A. V., Sukhikh, G. T., and Fatkhudinov, T. Kh. (2020). Macrophage Modification Strategies for Efficient Cell Therapy. Cells, 9(6), 1535. https://doi.org/10.3390/cells9061535

Porta, C., Riboldi, E., Ippolito, A., and Sica, A. (2015). Molecular and epigenetic basis of macrophage polarized activation. Seminars in Immunology, 27(4), 237–248. https://doi.org/10.1016/j.smim.2015.10.003

Ramírez-Labrada, A., Pesini, C., Santiago, L., Hidalgo, S., Calvo-Pérez, A., Oñate, C., … Pardo, J. (2022). All About (NK Cell-Mediated) Death in Two Acts and an Unexpected Encore: Initiation, Execution and Activation of Adaptive Immunity. Frontiers in Immunology, 13. Retrieved from https://www.frontiersin.org/articles/10.3389/fimmu.2022.896228

Rankin, L. C., and Artis, D. (2018). Beyond Host Defense: Emerging Functions of the Immune System in Regulating Complex Tissue Physiology. Cell, 173(3), 554–567. https://doi.org/10.1016/j.cell.2018.03.013

Richmond, A. (2002). NF-κB, chemokine gene transcription and tumour growth. Nature Reviews Immunology, 2(9), 664–674. https://doi.org/10.1038/nri887

Sakai, K., Kinoshita, T., and Matsumoto, K. (2014). Hepatocyte Growth Factor☆. In Reference Module in Biomedical Sciences. Elsevier. https://doi.org/10.1016/B978-0-12-801238-3.04055-1

Satoh, T., Takeuchi, O., Vandenbon, A., Yasuda, K., Tanaka, Y., Kumagai, Y., … Akira, S. (2010). The Jmjd3-Irf4 axis regulates M2 macrophage polarization and host responses against helminth infection. Nature Immunology, 11(10), 936-944. https://doi.org/10.1038/ni.1920

Sauter, K. A., Waddell, L. A., Lisowski, Z. M., Young, R., Lefevre, L., Davis, G. M., ... Hume, D. A. (2016). Macrophage colony-stimulating factor (CSF1) controls monocyte production and maturation and the steady-state size of the liver in pigs. American Journal of Physiology - Gastrointestinal and Liver Physiology, 311(3), G533-G547. https://doi.org/10.1152/ajpgi.00116.2016

Scaffidi, C., Fulda, S., Srinivasan, A., Friesen, C., Li, F., Tomaselli, K. J., … Peter, M. E. (1998). Two CD95 (APO-1/Fas) signaling pathways. The EMBO Journal, 17(6), 1675–1687. https://doi.org/10.1093/emboj/17.6.1675

Secchiero, P., Zerbinati, C., Rimondi, E., Corallini, F., Milani, D., Grill, V., ... Zauli, G. (2004). TRAIL promotes the survival, migration and proliferation of vascular smooth muscle cells. Cellular and Molecular Life Sciences: CMLS, 61(15), 1965–1974. https://doi.org/10.1007/s00018-004-4197-6

Secchiero, Paola, Gonelli, A., Mirandola, P., Melloni, E., Zamai, L., Celeghini, C., ... Zauli, G. (2002). Tumor necrosis factor-related apoptosis-inducing ligand induces monocytic maturation of leukemic and normal myeloid precursors through a caspase-dependent pathway. Blood, 100(7), 2421–2429. https://doi.org/10.1182/blood-2002-01-0047

Shi, C., and Pamer, E. G. (2011). Monocyte recruitment during infection and inflammation. Nature Reviews. Immunology, 11(11), 762–774. https://doi.org/10.1038/nri3070

Sica, A., and Mantovani, A. (2012). Macrophage plasticity and polarization: In vivo veritas. The Journal of Clinical Investigation, 122(3), 787–795. https://doi.org/10.1172/JCI59643

Sieweke, M. H., and Allen, J. E. (2013). Beyond Stem Cells: Self-Renewal of Differentiated Macrophages. Science, 342(6161), 1242974. https://doi.org/10.1126/science.1242974

Song, K., Chen, Y., Göke, R., Wilmen, A., Seidel, C., Göke, A., … Chen, Y. (2000). Tumor necrosis factor-related apoptosis-inducing ligand (TRAIL) is an inhibitor of autoimmune inflammation and cell cycle progression. The Journal of Experimental Medicine, 191(7), 1095–1104. https://doi.org/10.1084/jem.191.7.1095

Sprick, M. R., Rieser, E., Stahl, H., Grosse-Wilde, A., Weigand, M. A., and Walczak, H. (2002). Caspase-10 is recruited to and activated at the native TRAIL and CD95 death-inducing signalling complexes in a FADD-dependent manner but can not functionally substitute caspase-8. The EMBO Journal, 21(17), 4520–4530. https://doi.org/10.1093/emboj/cdf441

Stanley, E. R., Chen, D.-M., and Lin, H.-S. (1978). Induction of macrophage production and proliferation by a purified colony stimulating factor. Nature, 274(5667), 168–170. https://doi.org/10.1038/274168a0

Suzuki, A., Hanada, T., Mitsuyama, K., Yoshida, T., Kamizono, S., Hoshino, T., … Yoshimura, A. (2001). CIS3/SOCS3/SSI3 plays a negative regulatory role in STAT3 activation and intestinal inflammation. The Journal of Experimental Medicine, 193(4), 471–481. https://doi.org/10.1084/jem.193.4.471

Tang, D., Kang, R., Coyne, C. B., Zeh, H. J., and Lotze, M. T. (2012). PAMPs and DAMPs: Signal 0s that spur autophagy and immunity. Immunological Reviews, 249(1), 158–175. https://doi.org/10.1111/j.1600-065X.2012.01146.x

Tao, X., and Xu, A. (2016). Basic Knowledge of Immunology. In Amphioxus Immunity (pp. 15–42). Elsevier. https://doi.org/10.1016/B978-0-12-849903-0.00002-6

Tian, X., Tian, J., Tang, X., Ma, J., and Wang, S. (2016). Long non-coding RNAs in the regulation of myeloid cells. Journal of Hematology & Oncology, 9(1), 99. https://doi.org/10.1186/s13045-016-0333-7

Torraca, V., Cui, C., Boland, R., Bebelman, J.-P., van der Sar, A. M., Smit, M. J., … Meijer, A. H. (2015). The CXCR3-CXCL11 signaling axis mediates macrophage recruitment and dissemination of mycobacterial infection. Disease Models & Mechanisms, 8(3), 253–269. https://doi.org/10.1242/dmm.017756

Viola, A., Munari, F., Sánchez-Rodríguez, R., Scolaro, T., and Castegna, A. (2019). The Metabolic Signature of Macrophage Responses. Frontiers in Immunology, 10. Retrieved from https://www.frontiersin.org/articles/10.3389/fimmu.2019.01462

Vivier, E., and Malissen, B. (2005). Innate and adaptive immunity: Specificities and signaling hierarchies revisited. Nature Immunology, 6(1), 17–21. https://doi.org/10.1038/ni1153

Vogler, M., Dürr, K., Jovanovic, M., Debatin, K.-M., and Fulda, S. (2007). Regulation of TRAIL-induced apoptosis by XIAP in pancreatic carcinoma cells. Oncogene, 26(2), 248–257. https://doi.org/10.1038/sj.onc.1209776

von Karstedt, S., Montinaro, A., and Walczak, H. (2017). Exploring the TRAILs less travelled: TRAIL in cancer biology and therapy. Nature Reviews Cancer, 17(6), 352–366. https://doi.org/10.1038/nrc.2017.28

Wang, J., Chun, H. J., Wong, W., Spencer, D. M., and Lenardo, M. J. (2001). Caspase-10 is an initiator caspase in death receptor signaling. Proceedings of the National Academy of Sciences of the United States of America, 98(24), 13884–13888. https://doi.org/10.1073/pnas.241358198

Wang, N., Liang, H., and Zen, K. (2014). Molecular Mechanisms That Influence the Macrophage M1-M2 Polarization Balance. Frontiers in Immunology, 5. Retrieved from https://www.frontiersin.org/articles/10.3389/fimmu.2014.00614

Wang, Q., Ni, H., Lan, L., Wei, X., Xiang, R., and Wang, Y. (2010). Fra-1 protooncogene regulates IL-6 expression in macrophages and promotes the generation of M2d macrophages. Cell Research, 20(6), 701–712. https://doi.org/10.1038/cr.2010.52

Wang, X., Yao, B., Wang, Y., Fan, X., Wang, S., Niu, A., … Harris, R. C. (2017). Macrophage Cyclooxygenase-2 Protects Against Development of Diabetic Nephropathy. Diabetes, 66(2), 494–504. https://doi.org/10.2337/db16-0773

Wang, Y., Smith, W., Hao, D., He, B., and Kong, L. (2019). M1 and M2 macrophage polarization and potentially therapeutic naturally occurring compounds.

International Immunopharmacology, 70, 459–466. https://doi.org/10.1016/j.intimp.2019.02.050

Washburn, B., Weigand, M. A., Grosse-Wilde, A., Janke, M., Stahl, H., Rieser, E., ... Walczak, H. (2003). TNF-related apoptosis-inducing ligand mediates tumoricidal activity of human monocytes stimulated by Newcastle disease virus. Journal of Immunology (Baltimore, Md.: 1950), 170(4), 1814–1821. https://doi.org/10.4049/jimmunol.170.4.1814

Wei, W., Wang, D., Shi, J., Xiang, Y., Zhang, Y., Liu, S., ... Zheng, D. (2010). Tumor necrosis factor (TNF)-related apoptosis-inducing ligand (TRAIL) induces chemotactic migration of monocytes via a death receptor 4-mediated RhoGTPase pathway. Molecular Immunology, 47(15), 2475–2484. https://doi.org/10.1016/j.molimm.2010.06.004

Weisberg, S. P., McCann, D., Desai, M., Rosenbaum, M., Leibel, R. L., and Ferrante, A. W. (2003). Obesity is associated with macrophage accumulation in adipose tissue. The Journal of Clinical Investigation, 112(12), 1796–1808. https://doi.org/10.1172/JCI19246

Wiley, S. R., Schooley, K., Smolak, P. J., Din, W. S., Huang, C. P., Nicholl, J. K., ... Smith, C. A. (1995). Identification and characterization of a new member of the TNF family that induces apoptosis. Immunity, 3(6), 673–682. https://doi.org/10.1016/1074-7613(95)90057-8

Wu, Y., and Hirschi, K. K. (2021). Tissue-Resident Macrophage Development and Function. Frontiers in Cell and Developmental Biology, 8, 617879. https://doi.org/10.3389/fcell.2020.617879

Wynn, T. A., Chawla, A., and Pollard, J. W. (2013). Macrophage biology in development, homeostasis and disease. Nature, 496(7446), 445–455. https://doi.org/10.1038/nature12034

Xu, X., Huang, Q., Mao, Y., Cui, Z., Li, Y., Huang, Y., ... Li, W. (2012). Immunomodulatory effects of Bacillus subtilis (natto) B4 spores on murine macrophages. Microbiology and Immunology, 56(12), 817–824. https://doi.org/10.1111/j.1348-0421.2012.00508.x

Yao, Y., Xu, X.-H., and Jin, L. (2019). Macrophage Polarization in Physiological and Pathological Pregnancy. Frontiers in Immunology, 10. Retrieved from https://www.frontiersin.org/articles/10.3389/fimmu.2019.00792

Yin, M., Li, X., Tan, S., Zhou, H. J., Ji, W., Bellone, S., … Min, W. (2016). Tumor-associated macrophages drive spheroid formation during early transcoelomic metastasis of ovarian cancer. The Journal of Clinical Investigation, 126(11), 4157-4173. https://doi.org/10.1172/JCI87252

Zacchigna, L., Vecchione, C., Notte, A., Cordenonsi, M., Dupont, S., Maretto, S., … Bressan, G. M. (2006). Emilin1 Links TGF-β Maturation to Blood Pressure Homeostasis. Cell, 124(5), 929–942. https://doi.org/10.1016/j.cell.2005.12.035

Zagórska, A., Través, P. G., Lew, E. D., Dransfield, I., and Lemke, G. (2014). Diversification of TAM receptor tyrosine kinase function. Nature Immunology, 15(10), 920–928. https://doi.org/10.1038/ni.2986

Zhao, J., Yang, X., Auh, S. L., Kim, K. D., Tang, H., and Fu, Y.-X. (2009). Do adaptive immune cells suppress or activate innate immunity? Trends in Immunology, 30(1), 8–12. https://doi.org/10.1016/j.it.2008.10.003

Zhou, D., Huang, C., Lin, Z., Zhan, S., Kong, L., Fang, C., and Li, J. (2014). Macrophage polarization and function with emphasis on the evolving roles of coordinated regulation of cellular signaling pathways. Cellular Signalling, 26(2), 192–197. https://doi.org/10.1016/j.cellsig.2013.11.004

Zhou, D., Yang, K., Chen, L., Zhang, W., Xu, Z., Zuo, J., … Luan, J. (2017). Promising landscape for regulating macrophage polarization: Epigenetic viewpoint. Oncotarget, 8(34), 57693–57706. https://doi.org/10.18632/oncotarget.17027

Zhu, J., Zhou, Y., Wang, L., Hao, J., Chen, R., Liu, L., and Li, J. (2020). CXCL5/CXCL8 is a promising potential prognostic and tumor microenvironment-related cluster in hepatocellular carcinoma. Journal of Gastrointestinal Oncology, 11(6), 1364-1380. https://doi.org/10.21037/jgo-20-556

Ziegler-Heitbrock, L. (2007). The CD14+ CD16+ blood monocytes: Their role in infection and inflammation. Journal of Leukocyte Biology, 81(3), 584–592. https://doi.org/10.1189/jlb.0806510

Ziegler-Heitbrock, L., Ancuta, P., Crowe, S., Dalod, M., Grau, V., Hart, D. N., … Lutz, M. B. (2010). Nomenclature of monocytes and dendritic cells in blood. Blood, 116(16), e74–e80. https://doi.org/10.1182/blood-2010-02-258558

8. APPENDIX

8.1. Ethics Committee Approval

İZMİR BİYOTIP VE GENOM MERKEZİ
GİRİŞİMSEL OLMAYAN ARAŞTIRMALAR ETİK KURULU (İBG-GOEK)
KARARI

Toplantı Tarihi	: 25/06/2021	**Toplantı Günü**	: Cuma
Toplantı Sayısı	: 7	**Toplantı Saati**	: 10:30

Sayın Doç.Dr. Duygu SAĞ,

2021-017 Protokol No'lu; sorumlusu olduğunuz "DR4/5 ölüm reseptörü aktivasyonunun primer insan monositlerinin M1 makrofajlarına dönüşmesine etkisinin transkriptomik analizi" başlıklı araştırmanın uygulanmasında etik açıdan sakınca olmadığına oy birliği ile karar verilmiştir.

Bilgilerinizi ve gereğini rica ederiz.

Prof. Dr. H. Alper BAĞRIYANIK **Başkan**	**Dr. Serap ERKEK ÖZHAN** **Başkan Yardımcısı**
Prof. Dr. Sedef AKGÜNGÖR **Üye**	**Prof. Dr. İnci ALACALIOĞLU** **Üye**
Prof. Dr. Gülgün OKTAY **Üye**	**Prof. Dr. Hilmi ORHAN** **Üye**
Doç. Dr. Canan Aslı YILDIRIM **Üye**	

8.2. Curriculum Vitae

AYŞENUR ÖNER

Kişisel Bilgiler

İletişim Bilgileri

İletişim Adresi

Telefon

E-posta

İnternet Sayfası

Öğrenim Bilgileri

29 Eylül 2020 - Şu Anda (2 yıl 4 ay)
Yüksek Lisans, Tezli Program, DOKUZ EYLÜL ÜNİVERSİTESİ, TÜRKİYE
İZMİR ULUSLARARASI BİYOTIP VE GENOM ENSTİTÜSÜ, MOLEKÜLER BİYOLOJİ VE GENETİK (YL) (TEZLİ) (İNGİLİZCE)
Ağırlıklı Genel Not Ortalaması: 4.0 / 4.0

04 Ağustos 2015 - 16 Temmuz 2020 (5 yıl)
Lisans, Anadal/Normal Öğretim, İZMİR YÜKSEK TEKNOLOJİ ENSTİTÜSÜ, TÜRKİYE
FEN FAKÜLTESİ, MOLEKÜLER BİYOLOJİ VE GENETİK PR. (İNGİLİZCE)
Diploma Numarası: 4602
Ağırlıklı Genel Not Ortalaması: 3.48 / 4.0

Deneyim / İşyeri Bilgileri

01 Aralık 2021 - 01 Mayıs 2022 (6 ay) (Tam Zamanlı)
ARAŞTIRMACI, YÜKSEK LİSANS ÖĞRENCİSİ, NATIONAL UNIVERSITY OF IRELAND

01 Haziran 2019 - 01 Eylül 2019 (4 ay) (Tam Zamanlı)
STAJYER, UNIVERSITY MEDICAL CENTER GRONINGEN

01 Temmuz 2018 - 01 Ağustos 2018 (2 ay) (Tam Zamanlı)
STAJYER, İZMİR YÜKSEK TEKNOLOJİ ENSTİTÜSÜ FEN FAKÜLTESİ MOLEKÜLER BİYOLOJİ VE GENETİK BÖLÜMÜ

01 Haziran 2017 - 01 Ağustos 2017 (3 ay) (Tam Zamanlı)
STAJYER, İZMİR YÜKSEK TEKNOLOJİ ENSTİTÜSÜ FEN FAKÜLTESİ MOLEKÜLER BİYOLOJİ VE GENETİK BÖLÜMÜ

Yabancı Dil Bilgileri

İNGİLİZCE (Okuma: İyi, Yazma: İyi, Konuşma: İyi)

Ar-Ge Yetkinlik

Bildiriler

A. ÖNER, S. GÜNALP & D. SAČ WINGENDER, The effect of TRAIL-DR4/5 signaling activation on the differentiation of primary human monocytes into macrophages, Poster Sunumu, 5th International Molecular Immunology & Immunogenetics Congress, 20 Ekim 2022, 22 Ekim 2022.

R. ÖZBİLGİÇ, A. ÖNER, G. D. HELVACI, S. GÜNALP & D. SAČ WINGENDER, The Impact of CD95 Ligand (FasL) on Primary Human Macrophage Polarization, Poster Sunumu, International Cell Death Society, Future of Cell Death in Basic Science and Translational Medicine, 02 Temmuz 2022, 05 Temmuz 2022.

A. ÖNER, S. GÜNALP, G. D. HELVACI, A. KORKMAZ, G. WINGENDER & D. SAČ WINGENDER, The Effect of Ca2+ at a physiological concentration on primary human macrophage polarization, Poster Sunumu, 6th European Congress of Immunology, 01 Eylül 2021, 04 Eylül 2021.

TÜBİTAK Burs ve Destekleri

Proje Bilgileri

118Z997, TRAIL Aracılığı ile Gerçekleşen Sinyallerin İnsan iNKT Hücrelerinin Proliferasyonuna ve Fonksiyonlarına Etkisi, 1001 - Araştırma, Burslu, Sonuçlandı, ARDEB, KBAG - Kimya Biyoloji Araştırma Destek Grubu, Projeye Katılma/Ayrılma Tarihleri: 30.11.2020 - 28.02.2021, Proje Başlangıç/Bitiş Tarihleri: 01.03.2019 - 01.09.2021.

BİDEB Destekleri

AYŞENUR ÖNER, Etkinlik Destekleri ve Eğitim Bursları Müdürlüğü, 2210-A Genel Yurt İçi Yüksek Lisans Burs Programı, Bursu Kesildi, 2020 - 2, 01.10.2020 - 30.09.2022.

Panelistlik/İzleyicilik/Raportörlük Sayısı

Hakemlik/Panelistlik/Dış Danışmanlık Sayısı	ARDEB/BİDEB 0	TEYDEB 0	Toplam 0
İzleyicilik/Danışmanlık Sayısı	ARDEB/BİDEB 0	TEYDEB 0	Toplam 0
Raportörlük Sayısı	ARDEB/BİDEB 0	TEYDEB 0	Toplam 0